I. THE CALCULATION OF ATOMIC SCATTERING FACTORS
II. THE CRYSTAL STRUCTURE OF THE MICAS

Thesis by
Jack Sherman

In partial fulfillment of the requirements
for the degree of Doctor of Philosophy

California Institute of Technology
Pasadena, California
1932

Screening Constants for Many-electron Atoms. The Calculation and Interpretation of X-ray Term Values, and the Calculation of Atomic Scattering Factors.

By

Linus Pauling and J. Sherman in Pasadena.

(With 10 figures.)

The problem of the theoretical discussion of the properties of many-electron atoms and ions is a troublesome one, for it involves in every case a decision as to the extent to which rigor and accuracy are to be sacrificed to convenience. An accurate treatment of some properties of light atoms can be carried through. Thus Hylleraas[1]) has evaluated the energy of normal helium with great accuracy, and of other states with somewhat less accuracy, and the calculation of the polarizability of helium has also been reported[2]). But the methods used cannot be extended to heavy atoms because of the labor involved. The Thomas-Fermi[3]) atom is so simplified that it often does not give sufficient accuracy. Hartree's theory of the selfconsistent field[4]) gives the best values we have for electron distributions in heavy atoms; but this treatment is also very laborious, so that in the four years which have elapsed since it was originated only a few atoms have been treated, and, moreover, the discussion of every new property requires carrying out numerical or graphical calculations.

Moseley[5]), in his paper on the high-frequency spectra of the elements, expressed the frequencies of the K-lines which he had measured by the approximate equation

$$\nu = \frac{3}{4} R (Z - 1)^2 = (Z - 1)^2 R \left(\frac{1}{1^2} - \frac{1}{2^2}\right).$$

1) E. A. Hylleraas, Z. Physik **54**, 347. 1930; **65**, 209. 1930.

2) H. R. Hassé, Pr. Cambridge Phil. Soc. **26**, 542. 1930; J. C. Slater and J. G. Kirkwood, Physic. Rev. **37**, 682. 1931.

3) L. H. Thomas, Pr. Cambridge Phil. Soc. **23**, 542. 1927; E. Fermi, Z. Physik **48**, 73. 1928.

4) D. R. Hartree, Pr. Cambridge Phil. Soc. **24**, 89, 111. 1928.

5) H. G. J. Moseley, Phil. Mag. **26**, 1024. 1913.

In this equation, closely resembling the equation giving the frequencies of spectral lines of hydrogen-like atoms, the presence in the atom of electrons other than the emitting electron is taken into account by the use of a screening constant, here given the value 1. In further developing the theory of X-ray spectra Sommerfeld made continued use of the same procedure. He showed that the separations of the spin doublets were very well represented by his relativistic fine-structure equation for hydrogen-like atoms when suitable screening constants σ_2, independent of the atomic number, were introduced, and also pointed out that the main energy term could be similarly expressed, although the corresponding screening constants are not independent of the atomic number. A similar procedure was applied in the optical region with great success by Millikan and Bowen in their study of stripped atom spectra.

The simplicity of the calculation of the value of a physical property of a many-electron atom by this method is a strong argument in its favor. The theoretical discussion of most atomic phenomena is usually carried through first for hydrogen-like atoms, and often it is very difficult to extend the equations rigorously to atoms containing more than one electron. It would be pleasant if we could construct a single set of screening constants which on introduction in the appropriate hydrogen-like equation would deliver approximately correct values for any physical property of a many-electron atom. This possibility was eliminated, however, by Sommerfeld's early discovery[1]) that different screening constants must be used for different properties.

Five years ago one of us developed an approximate method for calculating screening constants, which was found to give values of the spin-doublet screening constant σ_2 in quite good agreement with those observed[2]). This led to the application of the same treatment in the discussion of other physical properties, the mole refraction, diamagnetic susceptibility, and sizes of a large number of atoms and ions[3]). It was found that the calculated screening constants for K and L electrons agreed well with experiment, but that for the succeeding shells there were increasingly large discrepancies arising from the approximations introduced in the theory. Of much greater importance than the calculation of individual screening constants was the discovery of a simple relation among the screening constants for various physical properties. This makes possible the construction of a single set of standard screening con-

1) A. Sommerfeld, Ann. Physik **51**, 125. 1916.
2) Linus Pauling, Z. Physik **40**, 344. 1926.
3) Linus Pauling, Pr. Roy. Soc. (A) **114**, 181. 1927.

stants, from which there can be easily obtained screening constants suitable for the discussion of any physical property of a large class, namely, those properties dependent mainly on the behaviour of the electrons in the outer parts of their orbits. In the following sections there is described such a standard set, obtained partially from theory, but mainly from empirical mole-refraction values and X-ray term values. It is shown that these constants lead to the complete interpretation of X-ray term values and optical ionization potentials. It is also found empirically that screening constants for an electron in a penetrating orbit are independent of the atomic number Z only as long as Z is so small as not to produce a large spin-relativity perturbation of the orbits of the electrons in the penetrated shells. The subsequent increase in their values is explained as resulting from the spin-relativity perturbation. In illustration of the use of the screening constants, a complete set of F-values, atomic scattering factors for X-rays, for atoms and ions is calculated with their aid.

There has recently been a recrudescence of interest in screening constants. Guillemin, Zener, and Eckart[1]) have applied variation methods to the wave equation to obtain approximate eigenfunctions for light atoms, in which screening constants occur as parameters, and Slater[2]) has suggested an empirical set of screening constants to be used in calculating various physical properties.

The Derivation of the Screening Constants.

The first set of screening constants was obtained from the discussion of the motion of an electron in the field of the nucleus and its surrounding electron shells, idealized as electrical charges uniformly distributed over spherical surfaces of suitably chosen radii. This idealization of electron shells was first used by Schrödinger[3]), and later by Heisenberg[4]) and Unsöld[5]), who pointed out that it is justified to a considerable extent by the quantum mechanics. The radius of a shell of electrons with principal quantum number n_i is taken as

1) V. Guillemin and C. Zener, Z. Physik **61**, 199. 1930; C. Zener, Physic. Rev. **36**, 50. 1930; C. Eckart, ibid. **36**, 878. 1930.

2) J. C. Slater, ibid. **36**, 57. 1930.

3) E. Schrödinger, Z. Physik **4**, 347. 1921.

4) W. Heisenberg, Z. Physik **39**, 499. 1926.

5) A. Unsöld, Ann. Physik **82**, 355. 1927.

$$\bar{r} = \int r \Psi\Psi^* d\tau = \gamma_i \frac{a_0 n_i^2}{Z} \tag{1}$$

with
$$\gamma_i = 1 + \frac{1}{2}\left\{1 - \frac{l_i(l_i+1)}{n_i^2}\right\}. \tag{2}$$

According to the old quantum theory, the orbit of an electron moving in such a field consists of a number of elliptical segments. Each segment can be characterized by a segmentary quantum number n_i, in addition to the azimuthal quantum number k, which is the same for all segments. In all cases it is found that about half of the entire orbit lies in the outermost ($_j$th) region.

Now many physical properties depend mainly on the behaviour of the electron in the outer part of its orbit. As an example we may mention the mole refraction or polarizability of an atom, which arises from deformation of the orbit in an external field. This deformation is greatest where the ratio of external field strength to atomic field strength is greatest; that is, in the outer part of the orbit. Let us consider such a property which for hydrogen-like atoms is found to vary with $n^r Z^{-t}$. Then a screening constant for this property would be such that

$$\text{const. } n_j^r Z_j^{-t} = \text{const. } n^r (Z - S)^{-t}.$$

It was found on expansion in powers of $\frac{z_i}{Z}$[1], neglecting all terms beyond the first, that

$$S = \sum_i z_i - \frac{r}{t} \sum_i z_i D_i \tag{3}$$

in which D_i, which is called the unit screening defect for an electron in the i^{th} shell, is given by the equation

$$D_i = \frac{1}{\pi}\{\beta_i u_i + (1 + \beta_i)\,\varepsilon \sin u_i\} - \beta_i \tag{4}$$

with
$$1 + \varepsilon \cos u_i = \frac{\gamma_i n_i^2}{n^2},$$

and
$$\beta_i = \frac{n^2}{\gamma_i n_i^2} - 1 .$$

From equation 3 it is seen that the total screening defect, that is, the difference between the number of screening electrons (those with principal quantum number equal to or less than that of the electron under consideration) and the screening constant, is proportional to $\frac{r}{t}$. For

1) z_i is the number of electrons in the i^{th} shell.

example, for a $1s$ electron screened by another $1s$ electron D_i is equal to 0.406. Now the energy of a penetrating electron is $Rh\frac{z_j^2}{n_j^2} = \frac{Rh(Z-S_E)^2}{n^2}$, so that S_E is given by equation (3) with $\frac{r}{t} = 1$. Hence S_E for a $1s$ electron is 0.594. The mole refraction is dependent essentially on n^6/Z^4, so that $\frac{r}{t} = 3/2$, and $S_R = 0.391$. The value of $\bar{r}$, that is, the size of the orbit, varies with n^2/Z, so that S_s, the size screening constant, is equal to 0.188. This shows how great the range of variation of screening constants for various properties is. It is probable that the relation found among the various screening constants holds with considerable accuracy even when the expression found for D_i is no longer accurate.

In the previous publication it was shown that the calculated screening constants for K and L electrons are in good agreement with the observed mole refraction values for helium and neon, so that in these cases the theory may be accepted as accurate. This result is not surprising. The idealization of electron shells as spherical surface charges is a reasonably good one for the inner electrons, as can be seen from their electron distribution functions, and the quantization of the orbit of the penetrating electron by the rules of the old quantum theory with the substitution of $\sqrt{l(l+1)}$ in place of the azimuthal quantum number k is also expected to give results closely approximating those which would be obtained from the quantum mechanics. For M, N, and O electrons the calculated screening constants are found on comparison with experiment to be too small, the error increasing in this order. This probably is due largely to the fact that the spherical-shell model is too strongly idealized for the outer electrons, whose distribution function does not show the rather sharp maximum of the inner shells. Accordingly for these electrons recourse must be made to empirical screening constants in constructing a standard set. The procedure followed is described in the next section.

The Screening Constants and their Use.

In fig. 1 and table I there are given size screening constants (with $\frac{r}{t}$ in equation 3 equal to 2) for all electrons in all neutral atoms. For K and L electrons the values given are the theoretical ones[1]). For M. N, and O electrons in atoms with rare-gas configurations the values given are those obtained from the measured mole refraction of argon, krypton,

1) A small numerical error in the values for $2s$ is corrected.

Table I.
Size Screening Constants[1]).

		1s	2s	2p	3s	3p	3d	4s	4p	4d	4f	5s	5p	5d	6s	6p	6d	7s
H	1	0																
He	2	0.19																
Li	3		1.25															
B	5			2.50														
Ne	10		3.10	4.57														
Na	11				6.6													
Al	13					8.7												
Ar	18				9.1	10.9												
K	19							13.4										
Ca	20				9.1	10.9		13.9										
Sc	21						14.7											
Zn	30				10.9	13.2	17.7	21.5										
Ga	31								24.4									
Kr	36							24.2	26.6									
Rb	37											30.4						
Sr	38							24.2	26.6			30.8						
Y	39									31.8		31.3						
Cd	48							25.6	28.4	34.0		37.0						
In	49												39.4					
Xe	54											38.8	41.8					
Cs	55														47			
Ba	56											38.8	41.8		47.4			
La	57							25.6	28.4	34.0				48.6	48			
Ce	58										43.0							
Lu	71							29.4	32.8	39.6	49.8	47.8	51.4	59	62			
Hg	80											50	54	62	66			
Tl	81															71.0		
Rn	86														67	72		
—	87																	80
Ac	89																81.0	
U	92	0.19	3.10	4.57	10.9	13.2	17.7	29.4	32.8	39.6	49.8	50	54	62	68	73	82	82.4

and xenon with the use of the calculated *s-p* separations, as described in the previous paper[2]). These values are extrapolated to smaller values of *Z*, for incomplete 8-shells, with the aid of the theoretical values. For $3s$, $3p$, and $3d$ in completed 18-shells the values obtained from the mole refraction of Zn^{++} with the calculated separations are retained. For $4s$, $4p$, $4d$ and $5s$, $5p$, $5d$ in 18-shells it was found from X-ray term

1) Screening constants for an atom not included in the table are to be obtained by linear interpolation. Thus S_s for a $2p$ electron for *C*, $Z = 6$, is $2.50 + \frac{1}{5}$ (4.57—2.50) = 2.91. 2) See note 3, p. 2.

Table Ia.

Electron Configurations of Atoms.

		$1s$	$2s$	$2p$	$3s$	$3p$	$3d$	$4s$	$4p$	$4d$	$4f$	$5s$	$5p$	$5d$	$6s$	$6p$	$6d$	$7s$
H	1	1																
He	2	2																
Li	3		1															
B	5		2	1														
Ne	10		2	6														
Na	11				1													
Al	13				2	1												
Ar	18				2	6												
K	19				2	6		1										
Ca	20				2	6		2										
Sc	21				2	6	1	2										
Zn	30				2	6	10	2										
Ga	31							2	1									
Kr	36							2	6									
Rb	37							2	6			1						
Sr	38							2	6			2						
Y	39							2	6	1		2						
Cd	48							2	6	10		2						
In	49							2	6	10		2	1					
Xe	54							2	6	10		2	6					
Cs	55							2	6	10		2	6		1			
Ba	56							2	6	10		2	6		2			
La	57							2	6	10		2	6	1	2			
Ce	58							2	6	10	1	2	6	1	2			
Lu	71							2	6	10	14	2	6	1	2			
Hg	80											2	6	10	2			
Tl	81														2	1		
Rn	86														2	6		
—	87														2	6		1
Ra	88														2	6		2
Ac	89														2	6	1	2
U	92	2	2	6	2	6	10	2	6	10	14	2	6	10	2	6	4	2

values (next section) that the calculated separations were somewhat too small, and so revised values are used, which, however, are in pretty good agreement with the observed mole refractions of 18-shell ions. The values given for $4s$, $4p$, $4d$, and $4f$ in the completed shell are from X-ray term values, while those for $6s$, $6p$, $6d$, and $7s$ are estimated. The electron configurations assumed (which differ slightly in some cases from those for the normal states of the neutral atoms) are given in table I a.

The screening constants for neutral atoms are constant so long as no additional screening electrons are introduced, as is strikingly shown by the energy screening constant for X-ray term values. But this con-

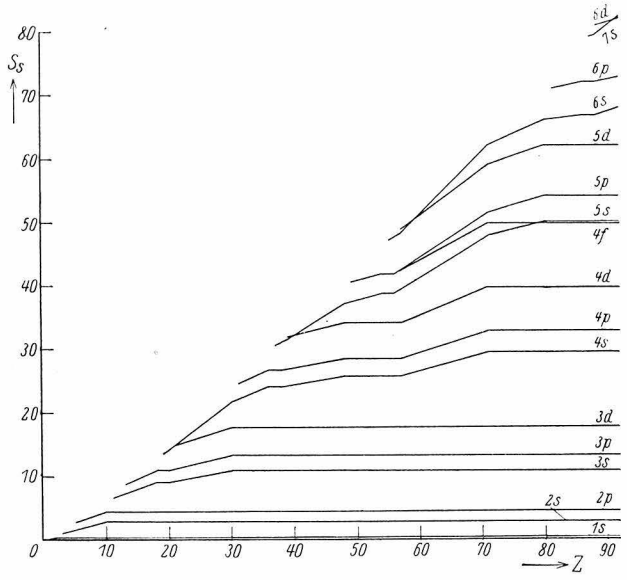

Fig. 1. Size screening constants S_S as functions of the atomic number Z.

stancy results in part from contributions of external electrons. It was found in the discussion of mole refraction of 8-shell atoms and ions that in an iso-electronic sequence the screening constant is in general a function of the atomic number, so that it can be written

$$S = S_0 - (Z - Z_0)\Delta S \tag{5}$$

in which S_0 is the value for the neutral atom with this configuration (and the atomic number Z_0), and ΔS has the values given in table II (for the size screening constant). This expression is to be

Table II.
The Size Screening Constant Correction for Ions.

Ion-type	Shell	Z_0		Ion-type	Z_0	Shell	
Ne	*L*	10	0.00				
Ar	*M*	18	0.07	Cu^+	28	*M*	0.07
Kr	*N*	36	0.25	Ag^+	46	*N*	0.30
Xe	*O*	54	0.50	Au^+	78	*O*	0.60
Rn	*P*	86	0.60				

used in obtaining screening constants for the outer electrons in ions. It is evident that it cannot hold when $Z—Z_0$ becomes very large, but is probably valid for actually occurring ions.

From this set of standard size screening constants it is possible to obtain screening constants for any atom or ion for any property dependent mainly on the behaviour of the electrons in the outer parts of their orbits. The constants can probably be trusted to be accurate to within about 10% of the quantum defect, for example, S_s values for M levels to within ± 1. In case that empirical data are available for some atoms or ions of a sequence it is well to use them to correct the screening constants.

Ionization Potentials and X-ray Term Values.

The energy of removal of an electron from an atom can be expressed in two ways by means of screening constants, either by taking the difference of $\sum_{i=1}^{n} \frac{(Z-S_i)^2}{n_i^2}$ for the neutral atom and $\sum_{i=1}^{n-1} \frac{(Z-S_i)^2}{n_i^2}$ for the ion, or by simply writing $I = \frac{(Z-S_E)^2}{n^2}$. The first of these methods, involving more arbitrary parameters, can be made more accurate, and, indeed, it seems in general to provide somewhat better values for the energy of removal of outer electrons than the second method. The two treatments give the same result for inner electrons, and for outer electrons in highly charged ions, in which cases the energy of rearrangement of the remaining electrons is negligible.

The energy of removal of an outer electron in a penetrating orbit is found with our treatment to be

$$I = \frac{(Z-S_E)^2}{n^2} \tag{6}$$

in Rydberg units of 13.53 Volt-electrons, in which S_E is given by equation 3 with $\frac{r}{t} = 1$. In table III there are given the experimental values of S_E for the removal of L electrons for various electron configurations of the atoms from *Li* to *Si*, together with the calculated values of S_E. Values of $Z—S_E$ are also plotted in figure 2. It is seen that in almost every sequence the empirical values approach the theoretical one asymptotically. This is strikingly shown by the six lithium-like ions and the five neon-like ions. Furthermore, for initial configurations with from one to five L electrons the empirical values are all in good agreement with the theoretical Moseley straight lines, but for more electrons there is pronounced deviation

Table III.
Values of the Energy Screening Constant S_E from Ionization Potentials.

Type of Ionization	Atom												Theoretical Values of S_E
	Li	*Be*	*B*	*C*	*N*	*O*	*F*	*Ne*	*Na*	*Mg*	*Al*	*Si*	
$2s$ from $1s^2\,2s$	1.740	1.684	1.658	1.644	1.637	1.633							1.626
$2s$ from $1s^2\,2s^2$		2.323	2.327	2.334									2.319
$2p$ from $1s^2\,2s^2\,2p$			3.43	3.32	3.26	3.23							3.244
$2p$ from $1s^2\,2s^2\,2p^2$				4.17	4.04	3.97							3.952
$2p$ from $1s^2\,2s^2\,2p^3$					4.93	4.78							4.660
$2p$ from $1s^2\,2s^2\,2p^4$						6.00	5.91						5.368
$2p$ from $1s^2\,2s^2\,2p^5$							6.76	6.52					6.076
$2p$ from $1s^2\,2s^2\,2p^6$								7.48	7.27	7.10	7.00	6.92	6.784

except for large Z. This deviation is to be attributed to the effect of the resultant spin as determined by Pauli's principle; when one electron is removed from a configuration with more than five L electrons, the multiplicity is increased instead of decreased.

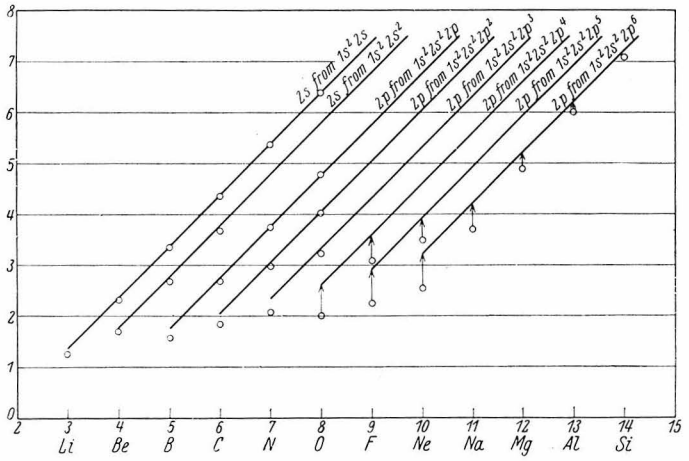

Fig. 2. Moseley diagrams for the energy of removal of an outer $2s$ or $2p$ electron. The straight lines give the theoretical values for large Z, the circles experimental values.

It has been shown[1]) that a similar treatment can be applied in the interpretation of X-ray term values by correcting for external screening with the aid of size screening constants. After correcting for the spin

1) L. Pauling and S. Goudsmit, "The Structure of Line Spectra". McGraw-Hill Book Co., New York, **1930**, pp. 187—191.

and relativity effects, the energy of removal of an inner electron from an atom may be written as

$$W = \frac{Rhc(Z-\sigma_1)^2}{n^2} = \frac{Rhc(Z-\sigma_0)^2}{n^2} - \sum_i \frac{z_i e^2}{\varrho_i a_0}, \tag{7}$$

in which σ_0 is equal to the energy screening constant S_E and the indicated summation is over the outer shells of electrons, each involving z_i electrons at an averate distance from the nucleus of ϱa_0. The customarily tabulated screening constant σ_1 is related to σ_0 by the equation

$$(Z-\sigma_1)^2 = (Z-\sigma_0)^2 - 2n^2 \sum_i \frac{z_i}{\varrho_i}. \tag{8}$$

$\varrho_i a_0$ is to be chosen in such a way as to give the right average value to $\frac{1}{r_i}$; that is

$$\frac{1}{\varrho_i a_0} = \left(\overline{\frac{1}{r_i}}\right).$$

For hydrogen-like states we have

$$\left(\overline{\frac{1}{r}}\right) = \frac{Z}{a_0 n^2},$$

so that from equation (3) we must place

$$\varrho_i = \frac{n_i^2}{Z - S_{S_i}}, \tag{9}$$

in which S_{s_i} is the size screening constant. Using the values of S_s given earlier, it was shown that the correction for external screening converts the empirical values of σ_1 which vary rapidly with Z into values of σ_0 which are effectively independent of Z.

But the relation between S_E and S_s given by equation (3) makes it possible to evaluate a complete set of screening constants from X-ray and optical term values alone. In view of the accuracy with which these term values can be measured and the completeness of the information they provide relative to all the electrons in all atoms, this method of obtaining screening constants must be considered as particularly valuable. The method of deriving the set is the following, illustrated with xenon. From the ionization potentials values of S_E for $5s$ and $5p$ are calculated by equation (6), and from them values of S_s. These are used in calculating S_E $(= \sigma_0)$ for $4s$, $4p$, and $4d$ from the empirical values of σ_1 given by the X-ray data for the N levels, using equations (8) and (9). The process is then repeated for the M, L, and K shells successively.

This treatment has not been systematically applied in constructing table I because of the lack of completeness of the X-ray term tables. It was accordingly necessary to assume a set of screening constants and test it by subsequent comparison of assumed and empirical S_E values. The empirical values of σ_1 are given in a figure on p. 460 of Sommerfeld's "Atombau und Spektrallinien," 4th edition. Their behaviour with changing Z is such as to make it absurd to call them screening constants. When the correction for external screening is made with the S_s values of table I,

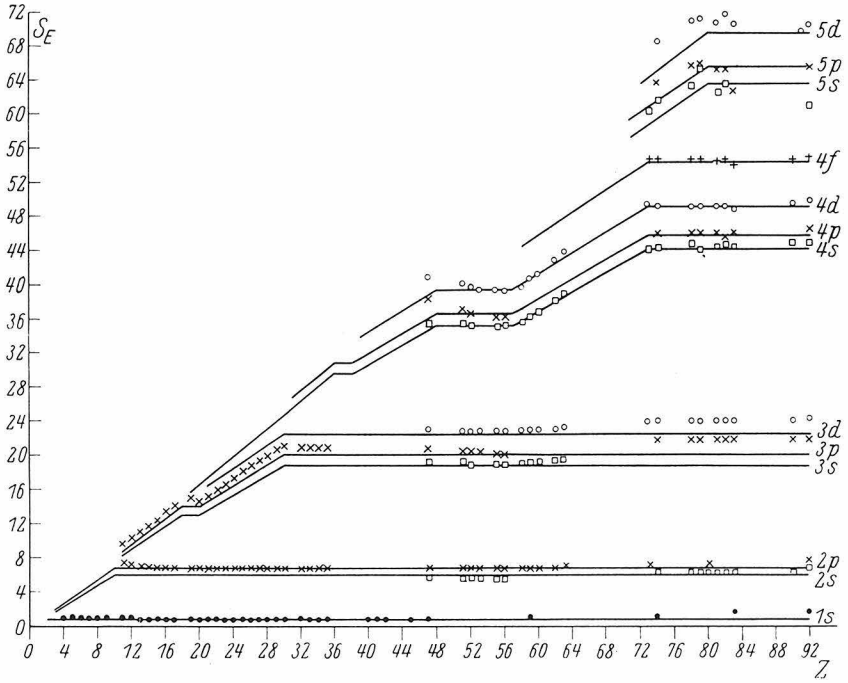

Fig. 3. Energy screening constants S_E as functions of the atomic number Z, compared with σ_0 values calculated from X-ray term values.

there result values of σ_0 which are practically independent of Z except when additional electrons are being introduced into inner shells. These σ_0 values are, moreover, in excellent general agreement with the S_E values obtained from table I by the use of equation (3), as is seen from figure 3.

In this calculation use was made of the reduced X-ray term values given by Wentzel[1]) for elements above silver, and of the K, L, and M term values for light elements given by Mukherjee and Ray[2]), corrected

1) G. Wentzel, Z. Physik **16**, 46. 1923.
2) B. C. Mukherjee and B. B. Ray, Z. Physik **57**, 345. 1929.

for fine structure with the use of the Sommerfeld equation. For K levels the fine-structure correction was made by inserting the value $\sigma_2 = 0.167$ in the expanded equation, using three terms for the heavier atoms.

It will be noticed from figure 3 and figure 4, in which σ_0 values for the $1s$ level are shown on a larger scale, that the σ_0 values agree well with S_E for light elements, but show an increasing deviation as the atomic number increases. This trend is found to be such that σ_0—S_E increases approximately with Z^3 or Z^4. This suggests at once that the spin-relativity correction has not been properly made; but on investigation it is found that this correction cannot be in error by an amount large enough to

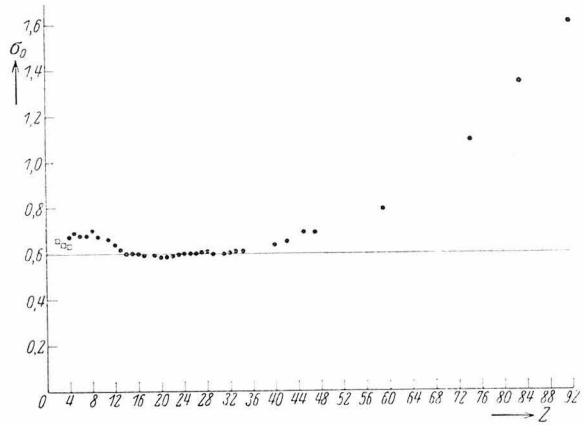

Fig. 4. Experimental σ_0 values. The circles are obtained from X-ray term values corrected for the spin-relativity effect and external screening, the squares from optical ionization potentials.

eliminate the trend in σ_0. Nor can the trend be due to error in the external screening correction, for even replacing the size screening constant S_s by the fine-structure screening constant σ_2, which is necessarily a safe lower limit for it, does not suffice to remove the trend. The explanation of the phenomenon is provided by the spin-relativity perturbations of the electron orbits, which cause all screening constants to be constants only for small values of Z, and then to increase with Z. The spin-relativity effect is for all electrons largest in the neighbourhood of the nucleus. As a result of this effect we expect an unusually large increase of the electron-density function $\psi\psi^*$ in the neighbourhood of the nucleus as Z increases, producing an extra ball of electricity near the nucleus, and hence increasing the screening constants for all electrons by about the same amount; and this increase should vary with Z^4. This expectation is

substantiated by the calculation of the electron distributions for $1s$ and $2s$ electrons according to Dirac's theory of the electron, using

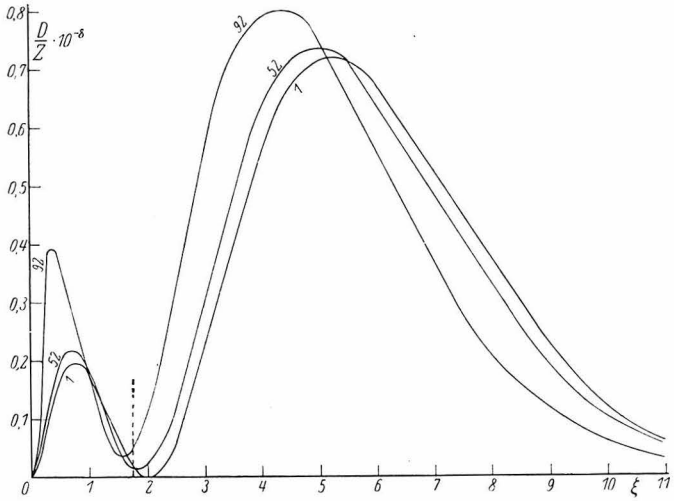

Fig. 5. The electron distribution function for a Dirac $2s$ electron in atoms with the indicated atomic numbers. The vertical broken line shows the position of $\bar{r}$ for a $1s$ electron.

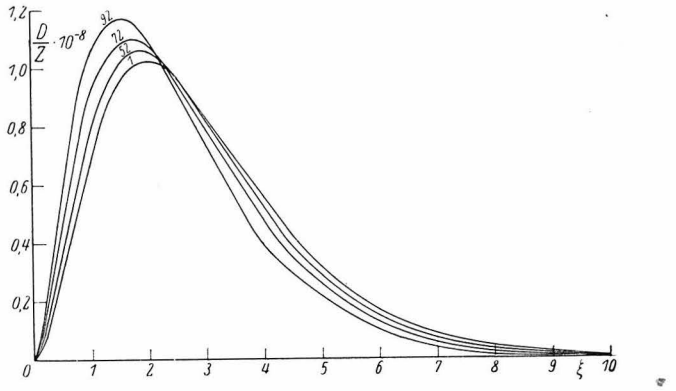

Fig. 6. The electron distribution function for a Dirac $1s$ electron in atoms with the indicated atomic numbers.

Gordon's complete solution[1]) of Dirac's equations. It is seen from figures 5 and 6 that the spin-relativity effect brings the electrons closer to the nucleus. The effect is particularly pronounced for $2s$ electrons,

1) W. Gordon, Z. Physik 48, 11. 1928. We are indebted to Mr. Sidney Weinbaum for the construction of figures 5 and 6.

in which case the small ball of electricity included within the first node of Schrödinger's eigenfunction is increased by about one-twentieth of an electron for $Z = 92$. This increase lies within the mean radius for $1s$ electrons, and so should be effective in increasing the $1s$ screening constants. It is probable that a similar and only slightly smaller concentration near the nucleus is shown also by the electrons in outer shells, so that the aggregate increase in the screening constant for $1s$ electrons may well reach the value 1 found empirically (increase from 0.6 to 1.6 for uranium). The effect should not be so pronounced for outer orbits, since these are already completely screened by certain inner shells, whose further concentration can have no influence.

This increase should be observed for all screening constants, and in particular for the Sommerfeld fine-structure screening constants. The constancy of s reported for the L-doublet throughout the periodic system ($s = 3.50 \pm 0.08$ from $Z = 41$ to $Z = 92$, Sommerfeld, "Atombau" pp. 447, 462) seems to contradict this. But actually this constancy proves the point. For s has been calculated with the complete formula,

$$\Delta\nu = R\left\{\frac{\alpha^2(Z-\sigma_2)^4}{2^4} + \frac{5\alpha^4(Z-\sigma_3)^6}{2^7} + \frac{53\alpha^6(Z-\sigma_4)^8}{2^{11}} + \ldots\right\}, \qquad (10)$$

by giving σ_2, σ_3, σ_4, ... the same value s. But σ_3, σ_4, ... which should have such values as to make $(Z - \sigma_3)^6$ equal to the mean value of $Z^6_{\text{effective}}$, are necessarily smaller than σ_2, since with increasing exponent the maximum values of $Z_{\text{effective}}$ become increasingly important. These higher terms are of considerable significance; for uranium $\frac{\Delta\nu_L}{R}$ is equal to 278, of which 75 is due to the higher terms. Accordingly Sommerfeld's values of s are actually mean values of σ_2 and σ_3, σ_4 ..., all of which are smaller than σ_2, and so decrease the mean. The values $\sigma_0 = 6.79$ and $\sigma_2 = 3.50$ suggest that σ_3, σ_4, ... are probably of the order of magnitude of 2. Assuming this value for uranium, it is found that the doublet separation leads to $\sigma_2 = 4.4$ instead of 3.5. Hence σ_2 also shows the spin-relativity increase, and the constancy of Sommerfeld's s is to be attributed to the fortuitous cancellation of this increase by the decrease produced by the inclusion in s of contributions by the smaller constants.

It is worthy of mention that the screening constants of table I and all those which can be derived from them satisfy an interval relation similar to that suggested for s by Sommerfeld; for a given total quantum number the intervals s—p, p—d, and d—f are in the ratios 1 : 2 : 3.

This relation is supported by the X-ray data as well as the theoretical calculations[1]).

F-Values for Hydrogen-like Eigenfunctions.

The scattering power of an electron distribution ϱ for the effective interplaner distance D given by the equation

$$\lambda = 2\,D \sin\,\Theta \tag{11}$$

or

$$D = \frac{d_{hkl}}{n} \tag{12}$$

is

$$F = \int_0^\infty \int_0^\pi \int_0^{2\pi} \varrho\, e^{2\pi i \frac{r}{D}\cos\Theta}\, r^2\, dr \sin\Theta d\Theta d\Phi\,, \tag{13}$$

in which r, Θ, and Φ are polar coordinates. We wish to evaluate F when ϱ is the electron distribution corresponding to the Schrödinger eigenfunctions for a hydrogen-like atom: i. e., for

$$\varrho_{nlm} = \Psi_{nlm}\,\Psi^*_{nlm}. \tag{14}$$

Instead of evaluating F_{nlm} for the individual eigenfunctions, let us average over the eigenfunctions corresponding to a subgroup; namely, over the $2\,l+1$ states with given n and l, and with $m = -l, -l+1, \ldots l-1, +l$. Since $\sum_m \Psi_{nlm}\,\Psi^*_{nlm}$ is independent of Θ and Φ, the electron distribution for a completed subgroup has spherical symmetry. With $\varrho = \varrho\,(r)$, equation (13) can at once be integrated over Φ and Θ, giving

$$F_{nl} = 2\,D \int_0^\infty \varrho_{nl}\,(r) \sin\frac{2\pi r}{D}\, r\, d\, r. \tag{15}$$

The averaged squared eigenfunction for a completed subgroup is

$$[\Psi_{nl}\,(r)]^2 = \frac{1}{2l+1} \sum_{m=-l}^{+l} \Psi_{nlm}\,(r, \Theta, \Phi)\,\Psi^*_{nml}\,(r, \Theta, \Phi)\,, \tag{16}$$

---

1) It may be mentioned that the neglect to take such an interval relation into consideration is the most pronounced defect of Slater's empirical set of screening constants (just as the arbitrary equating of the corresponding constant δ for $2\,s$ and $2\,p$ eigenfunctions is the most unsatisfactory part of Zener's variation treatment of the wave equation for light atoms). Thus Slater's screening constants for $3\,s$, $3\,p$, and $3\,d$ for an atom with completed K, L, and M shells are 11.6, 11.6, and 18, which may be compared with our values of 10.9, 13.2, and 17.7; the corresponding interval ratios p—s, d—p are 0:6.4 and 2.3:4.5. The effects of this unsatisfactory treatment of the $spdf$ sequence can be observed throughout Slater's discussion of applications of his screening constants.

with the value

$$\overline{\Psi}_{nl}(r) = \frac{1}{\sqrt{2\pi}} \left\{ \frac{(2\gamma)^{l+1}}{(n+l)!} \left(\frac{\gamma\,(n-l-1)!}{n\,(n+l)!} \right)^{\frac{1}{2}} \right\} e^{-\gamma r} r^l L_{n+l}^{2l+1}(2\gamma r), \tag{17}$$

in which

$$\gamma = \frac{4\pi^2 \mu e^2 Z}{n^2 h^2} = \frac{Z}{n\,a_0}, \tag{18}$$

with $a_0 = 0.529$ Å. The symbols are the customary ones (μ mass of electron, etc.).

$L_{n+l}^{2l+1}(2\gamma r)$ is an associated Laguerre polynomial, defined by the identity[1])

$$\sum_{\beta=0}^{\infty} \frac{L_{\alpha+\beta}^{\alpha}(\xi)}{(\alpha+\beta)!} u^{\beta} \equiv (-)^{\alpha} \frac{e^{\frac{-\xi u}{1-u}}}{(1-u)^{\alpha+1}}. \tag{19}$$

We are interested in integrating equation (15) with $\varrho_{nl}(r) = [\overline{\Psi}_{nl}(r)]^2$. It is convenient, however, to consider a more general class of integrals, in which

$$\varrho(r) = \varrho_{n_1 n_2 l}(r) = \overline{\Psi}_{n_1 l}(r)\,\overline{\Psi}_{n_2 l}(r). \tag{20}$$

Substituting this in equation (15), we obtain

$$F_{n_1 n_2 l} = \frac{D^{\frac{1}{2}}}{2} \left\{ (2\gamma_1)^{l+1} \left(\frac{\gamma_1 (n_1-l-1)!}{n_1 (n_1+l)!} \right)^{\frac{1}{2}} \right\} \left\{ (2\gamma_2)^{l+1} \left(\frac{\gamma_2 (n_2-l-1)!}{n_2 (n_2+l)!} \right)^{\frac{1}{2}} \right\} I_{n_1 n_2 l}(D), \tag{21}$$

in which γ_1 and γ_2 are given by equation (18) with $n = n_1$ and n_2 respectively, and $I_{n_1 n_2 l}(D)$ is the integral

$$I_{n_1 n_2 l}(D) = \int_0^{\infty} e^{-(\gamma_1+\gamma_2)r} \frac{L_{n_1+l}^{2l+1}(2\gamma_1 r)}{(n_1+l)!} \frac{L_{n_2+l}^{2l+1}(2\gamma_2 r)}{(n_2+l)!} J_{\frac{1}{2}}\left(\frac{2\pi r}{D}\right) r^{2l+\frac{3}{2}} dr. \tag{22}$$

In deriving this expression the factor $\sin \frac{2\pi r}{D}$ has been converted into a Bessel function of order $\frac{1}{2}$ by the known relation

$$\sin x = \sqrt{\frac{\pi x}{2}}\, J_{\frac{1}{2}}(x). \tag{23}$$

In order to evaluate the integrals $I_{n_1 n_2 l}(D)$ let us consider a function G defined by the identity

$$G = G_l(D, u, v) = \sum_{n_1=l+1}^{\infty} \sum_{n_2=l+1}^{\infty} I_{n_1 n_2 l}(D)\, u^{n_1-l-1} v^{n_2-l-1} \tag{24}$$

1) E. Schrödinger, Ann. Physik **80**, 484. 1926.

G is then a generating function for these integrals, which occur as coefficients in its expansion in powers of u and v; and it can be evaluated with the use of the generating function for the associated Laguerre polynomials, given in equation (19). Thus we have

$$G = \int_0^\infty e^{-(\gamma_1+\gamma_2)r} \sum_{n_1=l+1}^{\infty} \frac{L_{n_1+l}^{2l+1}(2\gamma_1 r)}{(n_1+l)!} u^{n_1-l-1} \sum_{n_2=l+1}^{\infty} \frac{L_{n_2+l}^{2l+1}(2\gamma_2 r)}{(n_2+l)!} v^{n_2-l-1}$$

$$\cdot J_{\frac{1}{2}}\left(\frac{2\pi r}{D}\right) r^{2l+\frac{3}{2}}\, dr = \int_0^\infty e^{-(\gamma_1+\gamma_2)r} \frac{(-)^{2l+1} e^{\frac{-2\gamma_1 r u}{1-u}}}{(1-u)^{2l+2}} \frac{(-)^{2l+1} e^{\frac{-2\gamma_2 r v}{1-v}}}{(1-v)^{2l+2}}$$

$$J_{\frac{1}{2}}\left(\frac{2\pi r}{D}\right) r^{2l+\frac{2}{3}}\, dr\,, \tag{25}$$

or, introducing the new variable

$$\zeta = \frac{Z}{a_0} r\,, \tag{26}$$

$$G = [(1-u)(1-v)]^{-2l-2} \left(\frac{a_0}{Z}\right)^{2l+\frac{5}{2}} \int_0^\infty e^{-\zeta\left[\frac{1}{n_1}\left(\frac{1+u}{1-u}\right)+\frac{1}{n_2}\left(\frac{1+v}{1-v}\right)\right]} J_{\frac{1}{2}}\left(\frac{2\pi a_0}{ZD}\zeta\right) \zeta^{2l+\frac{3}{2}}\, d\zeta\,. \tag{27}$$

This last integral is a special case of a more general integral which has before been found useful in quantum mechanical problems[1]). It was shown by Hankel and Gegenbauer that

$$\int_0^\infty e^{-a\zeta} J_\nu(z\zeta)\, \zeta^{\mu-1}\, d\zeta = \frac{\left(\frac{z}{2a}\right)^\nu \Gamma(\mu+\nu)}{a^\mu \Gamma(\nu+1)} F\left(\frac{\mu+\nu}{2}, \frac{\mu+\nu+1}{2}; \nu+1; -\frac{z^2}{a^2}\right), \tag{28}$$

where F denotes the hypergeometric function. Putting

$$a = \frac{1}{n_1}\left(\frac{1+u}{1-u}\right) + \frac{1}{n_2}\left(\frac{1+v}{1-v}\right),\ \nu = \tfrac{1}{2},\ z = \frac{2\pi a_0}{ZD},\ \text{and}\ \mu = 2l+\tfrac{5}{2},$$

this gives

$$G = [(1-u)(1-v)]^{-2l-2} \left(\frac{a_0}{Z}\right)^{2l+\frac{5}{2}} \frac{z^{\frac{1}{2}}\Gamma(2l+3)}{2^{\frac{1}{2}}\Gamma(\frac{3}{2})\, a^{2l+3}} F\left(l+\tfrac{3}{2}, l+2; \tfrac{3}{2}; -\frac{z^2}{a^2}\right) \tag{29}$$

1) B. Podolsky and Linus Pauling, Physic. Rev. **34**, 109. 1929.

the abbrevations z and a being retained for convenience. The hypergeometric series can be evaluated by the following method

$$\left.\begin{aligned} F\left(l+\tfrac{3}{2},\ l+2;\ \tfrac{3}{2};\ \frac{-z^2}{a^2}\right) &= 1-\frac{(l+\frac{3}{2})\,(l+2)}{1\cdot\frac{3}{2}}\,\frac{z^2}{a^2} \\ &\quad+\frac{(l+\frac{3}{2})\,(l+\frac{5}{2})\,(l+2)\,(l+3)}{1\cdot 2\cdot\frac{3}{2}\cdot\frac{5}{2}}\,\frac{z^4}{a^4}+\cdots \\ &= \sum_{t=0,2,4}^{\infty}\frac{(2l+2+t)!}{(2l+2)!\,(t+1)!}\left(\frac{iz}{a}\right)^t \\ &= \left(\frac{a}{iz}\right)\sum_{k=1,3,5,\ldots}^{\infty}\frac{(2l+2+k-1)!}{(2l+2)!\,k!}\left(\frac{iz}{a}\right)^k. \end{aligned}\right\} \tag{30}$$

Now the series given consists of just the alternate terms (the imaginary terms) in the expansion of $\left(1-\frac{iz}{a}\right)^{-2l-2}$. Hence we write

$$F\left(l+\tfrac{3}{2},\ l+2;\ \tfrac{3}{2};\ \frac{-z^2}{a^2}\right)=\frac{a}{z}\,\mathfrak{Im}\left[\left(1-\frac{iz}{a}\right)^{-2l-2}\right], \tag{31}$$

in which the symbol $\mathfrak{Im}$ means that only the imaginary part of the expression which follows it is to be retained. This leads to

$$G=\frac{D^{\frac{1}{2}}\,(2l+1)!}{\pi}\left(\frac{a_0}{Z}\right)^{2l+2} \mathfrak{Im}\left[\left(\frac{(1+u)\,(1-v)}{n_1}+\frac{(1-u)\,(1+v)}{n_2}-iz\,(1-u)\,(1-v)\right)^{-2l-2}\right]. \tag{32}$$

The problem is now solved. To find the F-value for the electron distribution of equation (20) with given n_1, n_2, and l, it is necessary to expand the bracketed expression in equation (32), to collect the imaginary terms, and multiply the coefficient of $u^{n_1-l-1}\,v^{n_2-l-1}$ by the factors given in equations (32) and (21).

The easiest way to obtain the coefficient of $u^{n_1-l-1}\,v^{n_2-l-1}$ is to differentiate n_1-l-1 times with respect to u, and n_2-l-1 times with respect to v. This causes all terms of lower degree in each auxiliary variable to vanish. Then by placing u and v equal to zero all terms of higher degree vanish, and the desired coefficient remains, multiplied by $(n_1-l-1)!\ (n_2-l-1)!$.

We are interested in the terms with $n_1=n_2=n$. With the introduction of the new variable

$$x=\frac{n\pi a_0}{ZD}, \tag{33}$$

Equations (21) and (32) lead to

$$F_{n,l}(x) = \frac{(2l+1)!}{2n\,(n+l)!\,(n-l-1)!}$$
$$x^{-1}\,\mathfrak{Im}\left[\frac{\hat{c}^{2n-2l-2}}{\hat{c}\,u^{n-l-1}\,\hat{c}\,v^{\cdot\,n-l-1}}\{1-uv-ix\,(1-u)\,(1-v)\}^{-2l-2}\right]$$
$$u=0,\ v=0. \tag{34}$$

Carrying out the indicated operations, there is obtained

$$\begin{aligned} F_{n,l}(x) = {} & \frac{1}{(n-l-1)!\,2n\,(1+x^2)^{2n}}\,(C_1^{n-l-1}\,(1+x^2)^{n-l-1} \\ & - C_2^{n-l-1}\,(n+l+1)\,(1+x^2)^{n-l-2}\,x^2 \\ & + C_3^{n-l-1}\,(n+l+1)\,(n+l+2)\,(1+x^2)^{n-l-3}\,x^4\ldots \\ & \ldots+(-1)^{n-l-1}\,C_{n-l}^{n-l-1}\,(n+l+1)\ldots\ldots(2n-1)\,x^{2(n-l-1)}) \\ & \cdot x^{-1}\,\mathfrak{Im}\,(1+ix)^{2n}, \end{aligned} \tag{35}$$

in which the coefficients C_r^{n-l-1} are numbers discussed later. The expression $(1+ix)^{2n}$ can now be expanded into a finite series and its imaginary part taken, with the result

$$\begin{aligned} x^{-1}\,\mathfrak{Im}\,(1+ix)^{2n} = {} & \binom{2n}{1} - \binom{2n}{3}x^2 + \binom{2n}{5}x^4 - \binom{2n}{7}x^6 + \ldots \\ & + (-)^{n+1}\binom{2n}{2n-1}x^{2n-2}, \end{aligned} \tag{36}$$

in which $\binom{2n}{1}$ etc. are binomial coefficients.

We can accordingly write

$$\begin{aligned} F_{n,l}(x) = {} & \frac{1}{(n-l-1)!}\,\{C_1^{n-l-1}\,(1+x^2)^{n-l-1} \\ & - C_2^{n-l-1}\,(n+l+1)\,(1+x^2)^{n-l-2}\,x^2 \\ & + C_3^{n-l-1}\,(n+l+1)\,(n+l+2)\,(1+x^2)^{n-l-3}\,x^4 - \ldots \\ & \ldots(-)^{n-l-1}\,C_{n-l}^{n-l-1}\,(n+l+1)\ldots(2n-1)\,x^{2(n-l-1)}\}\,F_{n,n-1}(x), \end{aligned} \tag{37}$$

in which

$$\begin{aligned} F_{n,n-1}(x) = {} & \frac{1}{2n\,(1+x^2)^{2n}}\left\{\binom{2n}{1} - \binom{2n}{3}x^2 + \ldots\right. \\ & \left. + (-)^{n+1}\binom{2n}{2n-1}x^{2n-2}\right\}. \end{aligned} \tag{37}$$

A table of binomial coefficients is given below (table IV). The numbers C_r^{n-l-1}, resulting from the successive partial differentiations, are given in table V, which can easily be extended with the use of the recursion formula

$$C_r^{n-l-1} = C_{r-1}^{n-l-2} + (2r-1)\, C_r^{n-l-2} + r^2\, C_{r+1}^{n-l-2} \tag{38}$$

or by the expression

$$C_r^{n-l-1} = \left\{\frac{(n-l-1)!}{(r-1)!}\right\}^2 \cdot \frac{1}{(n-l-r-1)!}. \tag{39}$$

We are indebted to Professor R. T. Birge of the Physics Department of the University of California for the discovery of the last expression.

Table IV.

Binomial Coefficients $\binom{2n}{\nu}$.

	$\nu = 1$	3	5	7	9	11	13
$2n = 0$	1						
$2n = 2$	2						
$2n = 4$	4	4					
$2n = 6$	6	20	6				
$2n = 8$	8	56	56	8			
$2n = 10$	10	120	252	120	10		
$2n = 12$	12	220	792	792	220	12	
$2n = 14$	14	364	2002	3432	2002	364	14

Table V.

Coefficients C_r^{n-l-1}.

	$r = 1$	2	3	4	5	6	7	8	9
$n-l-1 = 0$	1								
1	1	1							
2	2	4	1						
3	6	18	9	1					
4	24	96	72	16	1				
5	120	600	600	200	25	1			
6	720	4320	5400	2400	450	36	1		
7	5040	35280	52920	29400	7350	882	49	1	
8	40320	322560	564480	376320	117600	18816	1568	64	1

The Calculation of Atomic Scattering Factors.

Atomic scattering factors can now be calculated for any atom or ion by introducing in equation (37) the size screening constant for each electron as given in table I and summing over all electrons in the atom. Substitution of numerical values for the quantum numbers n and l in equation (37) gives the individual formulas of table VI. The seventeen functions corresponding to the eigenfunctions occupied in normal atoms were plotted on semi-log paper, with values of F as ordinates and of $\frac{1}{(Z-S_s)D}$ as logarithmic abscissae. This plot is reproduced in figure 7.

An inverse logarithmic scale was also constructed along the horizontal axis.

Table VI.

Formulas for F-values for hydrogen-like eigenfunctions

$$F_{1s} = \frac{1}{(1+x^2)^2}, \text{ with } x = \frac{n\pi a_0}{(Z-S_s)D}$$

$$F_{2p} = \frac{1-x^2}{(1+x^2)^4}. \qquad F_{2s} = (1-2x^2)F_{2p}$$

$$F_{3d} = \frac{(1-3x^2)(3-x^2)}{3(1+x^2)^6}. \quad F_{3p} = (1-4x^2)F_{3d}. \quad F_{3s} = (1-6x^2+3x^4)F_{3d}$$

$$F_{4f} = \frac{(1-x^2)(1-6x^2+x^4)}{(1+x^2)^8}. \; F_{4d} = (1-6x^2)F_{4f}. \; F_{4p} = (1-10x^2+10x^4)F_{4f}$$

$$F_{4s} = (1-12x^2+18x^4-4x^6)F_{4f}$$

$$F_{5g} = \frac{(5-60x^2+126x^4-60x^6+5x^8)}{5(1+x^2)^{10}} \qquad F_{5f} = (1-8x^2)F_{5g}$$

$$F_{5d} = (1-14x^2+21x^4)F_{5g}$$

$$F_{5p} = (1-18x^2+45x^4-20x^6)F_{5g}$$

$$F_{5s} = (1-20x^2+60x^4-40x^6+5x^8)F_{5g}$$

$$F_{6h} = \frac{(1-x^2)(3-52x^2+146x^4-52x^6+3x^8)}{3(1+x^2)^{12}}$$

$$F_{6d} = (1-24x^2+84x^4-56x^6)F_{6h}$$

$$F_{6p} = (1-28x^2+126x^4-140x^6+35x^8)F_{6h}$$

$$F_{6s} = (1-30x^2+150x^4-200x^6+75x^8-6x^{10})F_{6h}$$

$$F_{7j} = \frac{(7-182x^2+1001x^4-1716x^6+1001x^8-182x^{10}+7x^{12})}{7(1+x^2)^{14}}$$

$$F_{7s} = (1-42x^2+315x^4-700x^6+525x^8-126x^{10}+7x^{12})F_{7j}$$

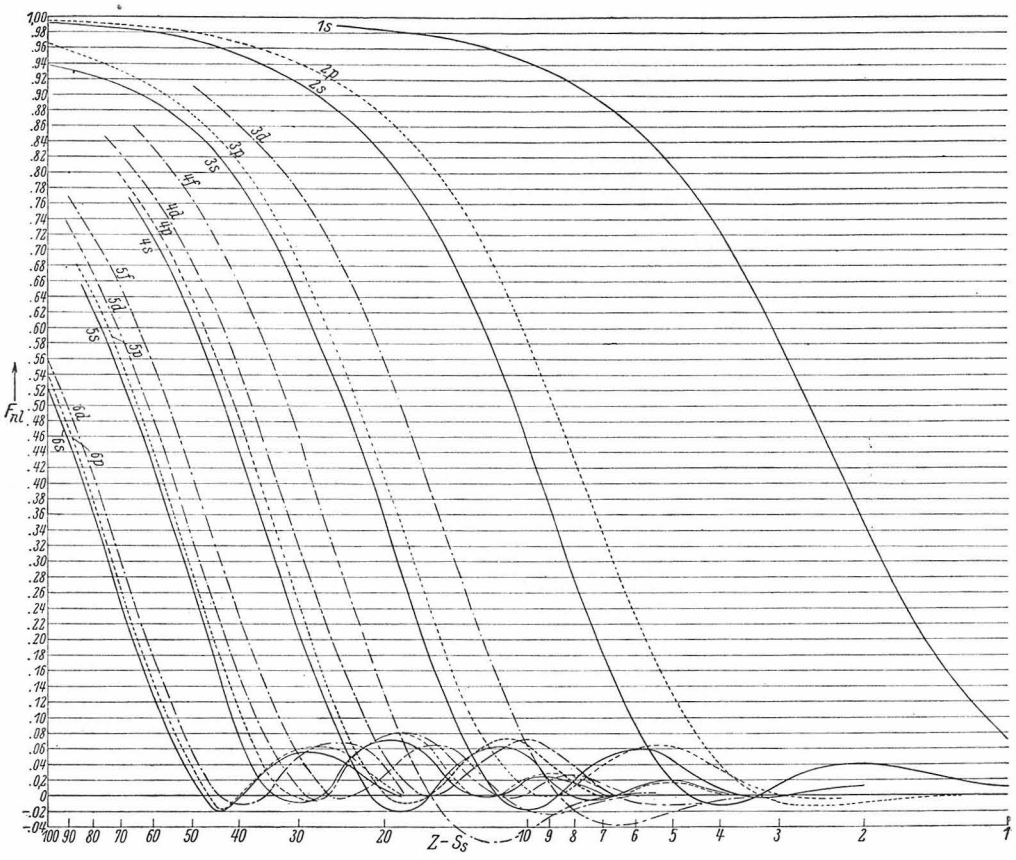

Fig. 7. F-values for hydrogen-like eigenfunctions.

With the aid of a movable template reproducing the horizontal scales, the values of F on a given curve for a given value of $Z—S_s$ and a series of values of D or of $\frac{\sin\Theta}{\lambda} = \frac{1}{2D}$ can be read from a single setting of the template, as is seen from the relation

$$\log\left(\frac{1}{(Z-S_s)\,D}\right) = -\log(Z-S_s) - \log D$$
$$= -\log(Z-S_s) + \log\frac{2\sin\Theta}{\lambda}. \qquad (40)$$

If the template is used as an inverse logarithmic scale, and is set at a given value of $Z—S_s$ on the inverse scale of the graph, then values of D on the template give the abscissae of the corresponding values of $\frac{1}{(Z-S_s)\,D}$.

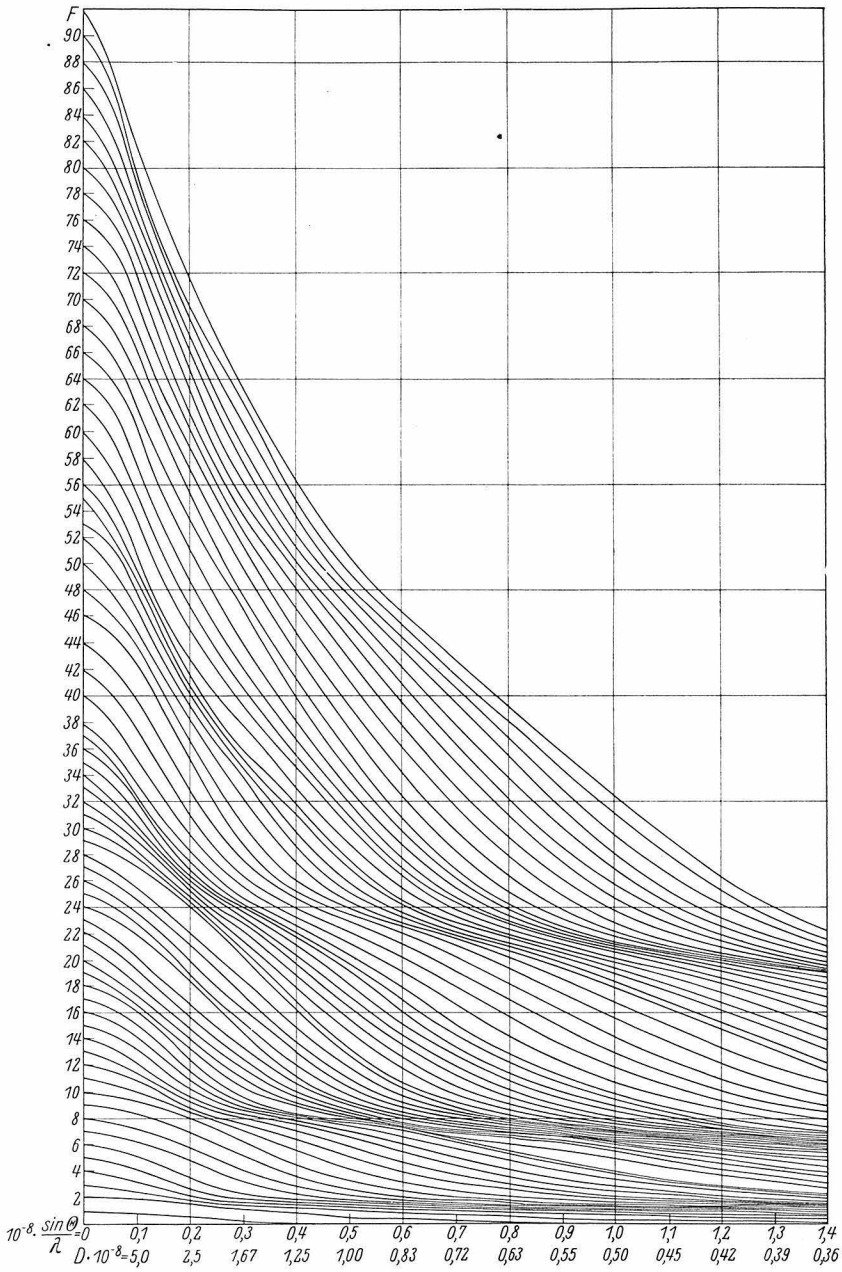

Fig. 8. F-values for neutral atoms.

If the template is used as a normal scale, and is set at a given value of $Z-S_s$ on the inverse scale of the graph, then values of $\frac{2\sin\Theta}{\lambda}$ on the template give the abscissae of the corresponding values of $\frac{1}{(Z-S_s)D}$.

Using the S_s values of table I, values of F for each electron in every atom from hydrogen to strontium and in every atom of even atomic number from strontium to uranium were obtained by this method for $10^8\frac{\sin\Theta}{\lambda}=0.0,\ 0.1,\ \ldots$ Atomic scattering factors were then found by taking the algebraic sum of the F-values for all electrons in the atom. These values are given in table VII, and are shown graphically in figure 8. Values of F similarly calculated for a number of ions are given in table VIII and figure 9.

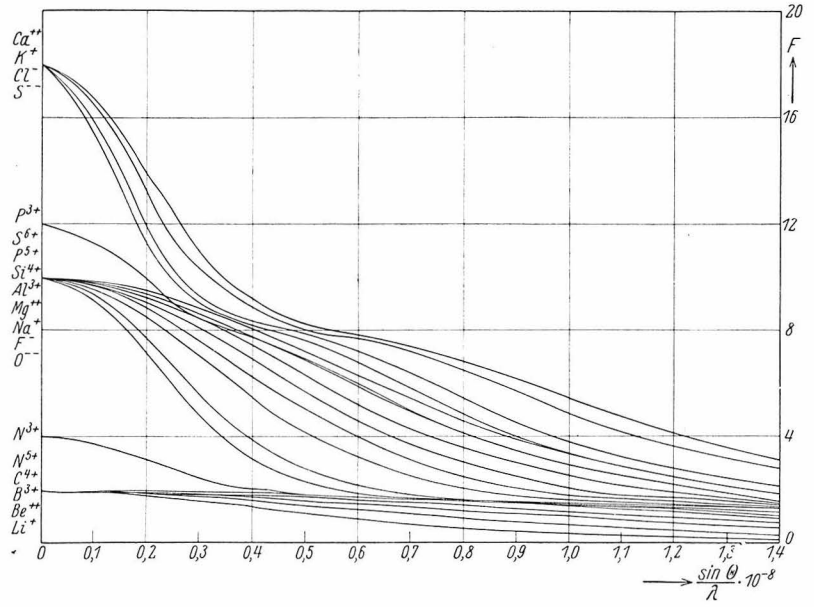

Fig. 9. F-values for ions.

These F-values are not so reliable as those calculated by Hartree's method. On the other hand, they are obtained with much less labor, Hartree's calculations having so far been carried out for only a small number of atoms. In figure 10 F-curves are shown for Li^+, Na^+, K^+, and Rb^+ as obtained by the method described in this paper, by Hartree's method and by the Thomas-Fermi method. It is seen that for all

Table VII. Scattering factors for atoms.

$\frac{\sin\theta}{\lambda} \cdot 10^{-8}$	0.0	0.1	0.2	0.3	0.4	0.5	0.6	0.7	0.8	0.9	1.0	1.1	1.2	1.3	1.4
H	1	0.81	0.48	0.25	0.13	0.07	0.04	0.03	0.02	0.01	0.01	0.00	0.00	0.00	0.00
He	2	1.86	1.55	1.17	0.84	0.54	0.40	0.29	0.21	0.15	0.12	0.09	0.07	0.05	0.04
Li	3	2.27	1.77	1.60	1.37	1.13	0.90	0.72	0.55	0.44	0.36	0.29	0.23	0.19	0.13
Be	4	3.19	2.10	1.73	1.61	1.48	1.31	1.13	0.94	0.82	0.68	0.57	0.48	0.41	0.34
B	5	4.16	2.73	1.96	1.69	1.59	1.49	1.39	1.26	1.11	0.97	0.87	0.75	0.65	0.57
C	6	5.21	3.62	2.42	1.86	1.66	1.57	1.51	1.42	1.32	1.21	1.10	0.99	0.89	0.79
N	7	6.32	4.76	3.26	2.33	1.86	1.65	1.55	1.50	1.43	1.36	1.27	1.17	1.09	0.99
O	8	7.36	5.82	4.14	2.90	2.19	1.80	1.63	1.54	1.49	1.44	1.38	1.31	1.23	1.15
F	9	8.42	6.95	5.17	3.66	2.69	2.10	1.77	1.61	1.51	1.47	1.43	1.38	1.35	1.28
Ne	10	9.47	8.09	6.29	4.62	3.37	2.57	2.05	1.77	1.60	1.51	1.47	1.43	1.39	1.35
Na	11	10.06	8.53	7.10	5.56	4.22	3.22	2.54	2.09	1.80	1.64	1.53	1.47	1.44	1.40
Mg	12	10.80	8.94	7.66	6.37	5.12	3.95	3.10	2.53	2.12	1.85	1.68	1.56	1.48	1.44
Al	13	11.50	9.32	8.11	7.05	5.89	4.72	3.74	3.04	2.54	2.15	1.87	1.70	1.60	1.51
Si	14	12.31	9.72	8.41	7.58	6.51	5.45	4.42	3.59	2.98	2.53	2.17	1.91	1.74	1.61
P	15	13.20	10.22	8.67	7.91	7.10	6.13	5.10	4.19	3.46	2.93	2.50	2.19	1.95	1.76
S	16	14.10	10.80	8.96	8.16	7.52	6.67	5.73	4.80	4.00	3.36	2.88	2.49	2.20	1.96
Cl	17	15.16	11.59	9.06	8.35	7.84	7.16	6.29	5.41	4.54	3.83	3.28	2.83	2.49	2.20
A	18	16.17	12.36	9.60	8.37	7.85	7.28	6.51	5.66	4.81	4.04	3.43	2.96	2.56	2.27
K	19	16.56	13.28	10.30	8.84	7.99	7.69	7.15	6.45	5.69	4.92	4.22	3.63	3.16	2.78
Ca	20	17.24	13.93	11.13	9.21	8.28	7.85	7.39	6.80	6.16	5.47	4.76	4.12	3.60	3.16
Sc	21	18.11	14.75	11.83	9.58	8.50	7.95	7.56	7.07	6.49	5.89	5.24	4.56	4.02	3.53
Ti	22	19.29	15.68	12.59	10.03	8.74	8.03	7.66	7.27	6.75	6.21	5.64	5.04	4.41	3.90
V	23	20.35	16.70	13.48	10.64	9.06	8.20	7.74	7.40	7.00	6.50	6.01	5.45	4.90	4.34
Cr	24	21.97	18.35	14.53	11.32	9.38	8.33	7.74	7.44	7.15	6.72	6.27	5.77	5.27	4.70
Mn	25	22.88	18.84	15.31	12.09	9.81	8.64	7.91	7.54	7.23	6.90	6.48	6.05	5.58	5.07
Fe	26	23.63	20.00	16.32	12.99	10.40	9.02	8.13	7.62	7.34	7.05	6.75	6.34	5.92	5.47
Co	27	24.60	21.05	17.37	13.87	10.98	9.33	8.33	7.70	7.37	7.11	6.84	6.49	6.11	5.69
Ni	28	25.55	22.16	18.50	14.85	11.79	9.77	8.60	7.87	7.44	7.20	6.97	6.68	6.34	5.97
Cu	29	27.28	24.03	20.09	16.08	12.80	10.29	8.89	7.97	7.41	7.14	6.93	6.71	6.42	6.07
Zn	30	27.90	24.36	20.76	16.88	13.53	10.84	9.26	8.26	7.61	7.22	7.02	6.79	6.55	6.25
Ga	31	28.50	24.84	21.58	17.89	14.57	11.81	9.85	8.67	7.87	7.34	7.04	6.83	6.61	6.36
Ge	32	29.20	25.24	22.30	18.84	15.52	12.70	10.51	9.16	8.22	7.57	7.12	6.88	6.69	6.45
As	33	29.87	25.61	22.90	19.75	16.44	13.59	11.30	9.72	8.64	7.87	7.33	6.96	6.74	6.55
Se	34	30.43	26.04	23.25	20.40	17.31	14.42	11.97	10.22	9.02	8.15	7.51	7.13	6.81	6.57
Br	35	31.20	26.40	23.72	21.24	18.24	15.23	12.81	10.89	9.54	8.57	7.82	7.26	6.88	6.59
Kr	36	32.48	26.87	24.04	21.86	19.03	16.09	13.53	11.54	10.04	9.00	8.16	7.54	7.07	6.72
Rb	37	32.70	27.49	24.23	22.20	19.71	16.89	14.22	12.15	10.47	9.34	8.44	8.16	7.47	7.15
Sr	38	33.36	28.34	24.64	22.58	20.37	17.70	15.13	12.89	11.11	9.77	8.85	8.11	7.53	7.08
Zr	40	35.15	29.61	25.54	23.27	21.36	19.07	16.62	14.36	12.34	10.77	9.56	8.72	8.03	7.49
Mo	42	37.67	31.06	26.35	24.04	22.25	20.22	17.96	15.66	13.66	11.83	10.48	9.37	8.59	7.95
Ru	44	39.90	32.89	27.46	24.62	22.95	21.23	19.17	17.03	14.98	13.12	11.47	10.18	9.21	8.46
Pd	46	42.52	35.22	28.77	25.17	23.46	22.07	20.34	18.32	16.21	14.25	12.53	11.06	9.89	8.99
Cd	48	43.89	36.60	30.36	25.98	23.85	22.52	21.18	19.42	17.43	15.52	13.75	12.46	10.84	9.77

Table VII (continuation).

$\frac{\sin\theta}{\lambda}\cdot 10^{-8}$	0.0	0.1	0.2	0.3	0.4	0.5	0.6	0.7	0.8	0.9	1.0	1.1	1.2	1.3	1.4
Sn	50	44.90	38.29	32.15	27.32	24.39	22.78	21.57	20.28	18.60	16.87	15.05	13.36	11.89	10.67
Te	52	46.62	37.44	34.06	28.82	25.33	23.22	21.94	20.75	19.45	17.87	16.30	14.65	13.05	11.69
I	53	47.42	39.83	34.70	29.60	25.85	23.56	22.13	20.97	19.77	18.39	16.84	15.28	13.66	12.27
Cs	55	49.00	40.87	35.91	31.22	26.99	24.19	22.43	21.28	20.19	18.96	17.62	16.22	14.81	13.34
Ba	56	49.42	41.58	35.54	32.08	27.73	24.66	22.78	21.56	20.48	19.38	18.11	16.69	15.31	13.92
Ce	58	50.98	43.11	37.75	33.29	29.03	25.52	23.31	21.87	20.83	19.82	18.72	17.49	16.14	14.76
Nd	60	53.27	45.20	39.28	34.66	30.22	26.40	23.81	22.15	21.11	20.14	19.20	18.09	16.95	15.68
Sa	62	55.38	47.10	40.64	35.63	31.00	27.06	24.29	22.58	21.47	20.59	19.67	18.71	17.66	16.43
Gd	64	57.58	49.11	42.16	36.78	31.97	27.78	24.78	22.88	21.66	20.83	20.00	19.16	18.16	17.10
Dy	66	58.40	51.33	44.11	38.24	33.22	28.81	25.45	23.32	21.91	21.04	20.29	19.53	18.66	17.72
Er	68	61.93	53.45	46.66	39.70	34.45	29.83	26.17	23.79	22.26	21.29	20.60	19.88	19.12	18.22
Yb	70	64.06	55.71	47.78	41.30	35.81	30.93	26.94	24.23	22.49	21.40	20.75	20.06	19.43	18.59
Hf	72	66.05	57.58	49.71	43.16	37.62	32.45	28.25	25.10	22.96	21.67	20.81	20.16	19.60	18.98
W	74	67.81	58.84	51.06	44.96	39.33	34.24	29.77	26.33	23.80	22.10	20.95	20.23	19.62	18.97
Os	76	69.64	60.33	52.33	46.67	41.26	36.12	31.51	27.73	24.86	22.76	21.42	20.41	19.73	19.17
Pt	78	72.27	61.92	53.43	48.12	43.01	38.00	33.13	29.12	26.06	23.72	22.07	20.81	19.96	19.36
Hg	80	73.84	63.48	54.68	49.25	44.49	39.50	34.93	30.68	27.22	24.89	22.75	21.34	20.28	19.45
Pb	82	74.93	65.08	56.10	50.02	45.61	40.93	36.39	32.25	28.51	25.57	23.47	21.84	20.66	19.82
Po	84	76.14	66.58	57.74	51.16	46.61	42.16	37.90	33.81	29.97	26.78	24.30	22.51	21.13	20.11
Rn	86	77.64	67.86	59.43	52.19	47.55	43.38	39.28	35.37	31.53	28.12	25.30	23.19	21.67	20.48
Ra	88	78.80	68.77	60.85	53.47	48.23	44.46	40.43	36.72	33.06	29.59	26.58	24.11	22.30	20.96
Th	90	79.73	69.77	62.19	55.04	49.31	45.49	41.63	37.99	34.56	31.09	27.99	25.26	23.11	21.51
U	92	80.75	71.38	63.36	56.46	50.42	46.16	42.69	39.07	35.72	32.47	29.30	26.41	23.96	22.21

Table VIII. Scattering factors for ions.

$\frac{\sin\theta}{\lambda}\cdot 10^{-8}$	0.0	0.1	0.2	0.3	0.4	0.5	0.6	0.7	0.8	0.9	1.0	1.1	1.2	1.3	1.4
Li^{+}	2.00	1.94	1.78	1.58	1.33	1.09	0.88	0.70	0.54	0.43	0.35	0.28	0.23	0.18	0.13
Be^{++}	2.00	1.97	1.88	1.75	1.59	1.41	1.23	1.06	0.91	0.77	0.65	0.54	0.46	0.39	0.33
B^{3+}	2.00	1.98	1.92	1.84	1.72	1.60	1.45	1.32	1.18	1.04	0.92	0.81	0.70	0.61	0.54
C^{4+}	2.00	1.99	1.95	1.88	1.80	1.70	1.60	1.49	1.37	1.25	1.13	1.03	0.92	0.83	0.74
N^{5+}	2.00	1.99	1.96	1.91	1.85	1.78	1.69	1.60	1.51	1.41	1.31	1.21	1.11	1.02	0.93
N^{3+}	4.00	3.73	3.12	2.47	2.02	1.79	1.66	1.59	1.54	1.46	1.38	1.29	1.19	1.09	1.00
$O^{=}$	10.00	9.15	7.07	4.84	3.22	2.32	1.83	1.61	1.51	1.46	1.42	1.37	1.29	1.22	1.14
F^{-}	10.00	9.33	7.65	5.61	3.90	2.80	2.14	1.78	1.60	1.50	1.46	1.42	1.37	1.34	1.27
Na^{+}	10.00	9.60	8.54	7.06	5.49	4.19	3.25	2.54	2.09	1.79	1.63	1.53	1.46	1.43	1.39
Mg^{++}	10.00	9.70	8.86	7.65	6.26	5.02	3.92	3.10	2.53	2.12	1.84	1.66	1.55	1.46	1.42
Al^{3+}	10.00	9.77	9.08	8.10	6.90	5.72	4.63	3.71	3.04	2.54	2.15	1.87	1.69	1.58	1.49
Si^{4+}	10.00	9.81	9.25	8.42	7.41	6.28	5.27	4.31	3.57	2.98	2.55	2.18	1.91	1.73	1.59
P^{5+}	10.00	9.85	9.37	8.67	7.79	6.82	5.84	4.93	4.11	3.44	2.94	2.52	2.21	1.95	1.76
P^{3+}	12.00	11.30	9.85	8.68	7.79	6.91	5.97	5.01	4.15	3.45	2.93	2.51	2.21	1.96	1.77
S^{6+}	10.00	9.88	9.47	8.86	8.09	7.22	6.31	5.44	4.64	3.92	3.34	2.89	2.51	2.22	1.98
$S^{=}$	18.00	15.50	11.20	8.97	8.21	7.64	6.79	5.81	4.84	4.02	3.37	2.87	2.49	2.19	1.96

Table VIII (continuation).

$\frac{\sin\theta}{\lambda} \cdot 10^{-8}$	0.0	0.1	0.2	0.3	0.4	0.5	0.6	0.7	0.8	0.9	1.0	1.1	1.2	1.3	1.4
Cl^-	18.00	15.90	11.90	9.31	8.36	7.89	7.22	6.35	5.44	4.56	3.84	3.28	2.83	2.49	2.20
K^+	18.00	16.50	13.20	10.30	8.80	7.98	7.69	7.15	6.45	5.69	4.92	4.22	3,63	3.16	2.78
Ca^{++}	18.00	16.80	13.90	11.00	9.22	8.26	7.81	7.37	6.79	6.16	5.47	4.76	4.12	3.60	3.16
Rb^+	36.00	32.64	27.44	24.22	22.19	19.71	16.89	14.22	12.15	10.47	9.34	8.44	8.16	7.47	7.15

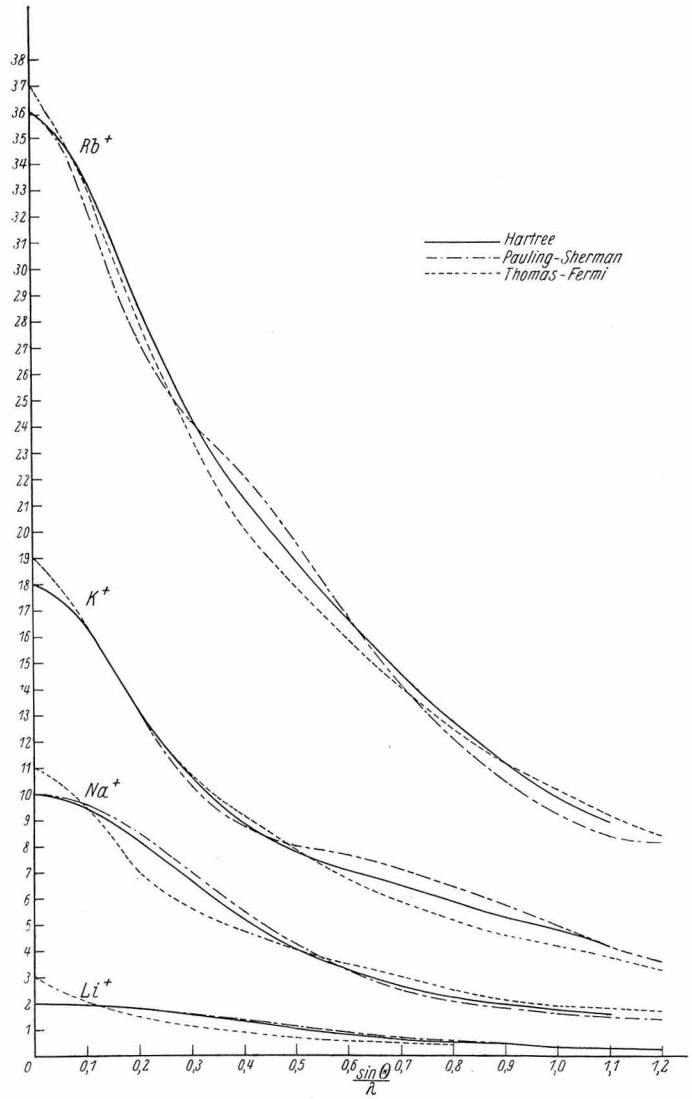

Fig. 10. Comparison of Hartree, Pauling-Sherman, and Thomas-Fermi F-values for Li^+, Na^+, K^+, and Rb^+. (Thomas-Fermi values are for neutral atoms.)

atoms there is good agreement between the values of this paper and those of Hartree, the maximum difference being 0.3 for Na^+ and 1.2 for Rb^+. The agreement between the Thomas-Fermi values and Hartree's is nearly as good for heavy atoms, but not good for light ones, on account of the approximations involved in the Thomas-Fermi statistical treatment. It is of interest to note the effect of the completed K, L, M etc. shells in causing the Pauling-Sherman curves to vary from one side to the other of the Thomas-Fermi curves. The Hartree curves behave in the same way, but the waves are not so pronounced, inasmuch as the nodes in the eigenfunctions, neglected completely in the Thomas-Fermi treatment, have been over-emphasized in using hydrogen-like eigenfunctions. For this reason the Hartree curves usually lie between the Thomas-Fermi and Pauling-Sherman curves, and for heavy atoms the mean of the Thomas-Fermi and Pauling-Sherman values is probably somewhat better than either set alone.

The effect of the K, L, and M shells in successive atoms is strikingly shown in figures 9 and 10 by the concentration of the curves in certain regions.

Summary.

After a discussion of screening constants and their uses, in which the relation between screening constants for various physical properties is presented, it is pointed out that a complete set of screening constants could be obtained from X-ray term values and ionization potentials alone. In default of complete knowledge of term values and ionization potentials of heavy atoms, a table of size screening constants for all electrons in all atoms has been prepared partially from theoretical calculations and partially from term values. It is shown that this table of screening constants permits a satisfactory detailed interpretation of energy levels of atoms. The screening constants for inner electrons are found not to be constant but to increase rapidly for large values of the atomic number. The phenomenon is interpreted as a spin-relativity effect with the aid of Dirac's theory of the electron.

A general expression for the scattering factor for X-rays of a hydrogen-like eigenfunction has been obtained. By substituting screening constants in it, F-values for atoms and ions have been obtained which show good agreement with those calculated by Hartree's method.

July 28, 1931. Gates Chemical Laboratory, California Institute of Technology.

Received August 17th, 1931.

THE CRYSTAL STRUCTURE OF THE MICAS

I. Introduction

The micas represent an extensive class of monoclinic (pseudohexagonal) minerals occurring in nature. They possess the striking physical property of excellent basal cleavage which permits the separation of very thin elastic lamellae.

Aside from the measurements of interplanar distances normal to the plane of cleavage, the X-ray study of these minerals has been reported by Mauguin (1) and by Jackson and West (2). Mauguin prepared and analyzed Laue and rotation photographs, obtaining the size of the unit and the space group for various micas; he did not obtain the atomic arrangement. During the course of the present investigation, Jackson and West published a paper in which they report the structure of mica, their results being in agreement with those found here.

In this investigation, muscovite, corresponding approximately to the chemical composition $KAl_3Si_3O_{10}(OH)_2$ was studied in detail.

II. The Unit of Structure and Space Group

Oscillation photographs for the determination of the lattice constants were made with molybdenum K-radiation reflected from the pinacoids. The data for (001) are given in table I. The data lead to a unit with $d_{100}/n_1 = 2.59$ Å, $d_{010}/n_2 = 4.50$ Å, $d_{001}/n_3 = 10.02$ Å $\beta = 96°$. n_1, n_2, and n_3 are the orders of reflection of the first lines on the respective photographs. Laue photographs were taken with the indident beam of X-rays normal to (001), the plane of cleavage, of a crystal of fuchsite, (a variety of muscovite), and of lepidolite, a lithium-containing mica. The short wave length limit of X- radiation present in the incident beam was 0.24 Å. The smallest unit which will give calculated values of $n\lambda$ not less than 0.24 Å for all Laue spots is that corresponding to $n_1 = n_2 = n_3 = 2$. Since this unit accounts for all reflections observed on the three Laue photographs which were analyzed, it is to be accepted as the correct one. Table II lists the first order reflections from the fuchsite photograph. (on the three photographs analyzed a total of approximately one hundred fifty forms reflected).

Table I

Measurement of d_{001}/n_3

Order	Line	θ	d_{001}/n_3
$2n_3$	α	4° 3'13"	10.03
$3n_3$	α	6° 6'38"	9.99
$4n_3$	α	8° 7'49"	10.03
$5n_3$	α_1	10° 10'43"	10.03
$6n_3$	α_1	12° 13'37"	10.04
$7n_3$	α_1	14° 16'31"	10.03
$8n_3$	α_1	16° 23'12"	10.04
$8n_3$	α_2	16° 23'28"	10.04
$9n_3$	α_1	18° 33'43"	10.02
$10n_3$	α_1	20° 30' 0"	10.04
$10n_3$	α_2	20° 45'18"	10.05
$11n_3$	α_1	22° 55' 8"	10.01
$12n_3$	α_1	25° 3'43"	9.99
$12n_3$	α_2	25° 20' 0"	9.98
$13n_3$	α_1	27° 25' 0"	9.99
$13n_3$	α_2	27° 35'13"	9.99
$15n_3$	α_1	32° 3'54"	10.00
$18n_3$	α_1	39° 27'43"	10.02
$18n_3$	α_2	39° 45'43"	10.02

average: 10.02

Table II.

First Order Reflections from a Laue Photograph of Fuchsite

X-ray Beam Normal to (001). 160 mah.

Form {hkl}	nλ Å
061	.27, .30
083	.32, .41
130	.25
310	.34, .37
151	.33, .48
172	.31, .32, .43
173	.34, .45
174	.48, .48
193	.28, .38
194	.32, .39
195	.38, .46
1·11·7	.42, .48
263	.41
283	.36, .44
285	.38, .46
2·12·9	.36, .41

Table II, Continued

Form {hkl}	nλ Å
313	.46, .48
375	.34, .41
376	.43
395	.42, .48
397	.43, .47
398	.42, .48
415	.46, .48
445	.37, .41
487	.33
489	.44
517	.45, .46
535	.25, .28
536	.36, .38
557	.34, .38
559	.46
577	.32
59·10	.34, .37
59·11	.38, .41
66·11	.39, .42
715	.42, .42

The fundamental translations are:

$d_{100} = 5.19$ Å; $d_{010} = 8.99$ Å; $d_{001} = 20.04$ Å

These are confirmed by the application of the Polanyi formula to the layer lines occurring on all oscillation photographs. The lengths of the axes are:

$\underline{a} = d_{100}/\sin\beta = 5.19/\sin 96^\circ = 5.23$ Å

$\underline{b} = d_{010} = 8.99$ Å

$\underline{c} = d_{001}/\sin\beta = 20.04/\sin 96^\circ = 20.14$ Å

The axial ratios $\underline{a} : \underline{b} : \underline{c}$ are 0.582 : 1 : 2.24. These may be compared with the axial ratios given by Dana: $\underline{a}_{Dana} : \underline{b}_{Dana} : \underline{c}_{Dana} = 0.57735 : 1 : 3.3128$, $\beta = 89^\circ 54'$. Hence, $\underline{a}_{Dana} : \underline{b}_{Dana} : \underline{c}_{Dana} = 0.57735 : 1 : \frac{3}{2} \cdot 2.208$.

In calculating the interplanar distances for the interferences on the Laue photographs, the following formula was used:

$$d_{hk\ell} = \frac{b}{\sqrt{\frac{\left(\frac{h}{\frac{a}{b}}\right)^2 + \left(\frac{\ell}{\frac{c}{b}}\right)^2 - \frac{2h\ell\cos\beta}{\frac{ac}{b^2}}}{\sin^2\beta} + K^2}}$$

Substituting in the values for $\underline{a}$, $\underline{b}$, $\underline{c}$, and β

$$d_{hk\ell} = \frac{8.99}{\sqrt{3.034\ h^2 + 0.2015\ell^2 + 0.1634\ h\ell + k^2}}$$

Assuming 3, 4, and 5 molecules of muscovite, $KAl_3Si_3O_{10}(OH)_2$, to the unit cell, the calculated densities are 2.11, 2.82, and 3.52 gms/cc, respectively. The density given by Dana for mica is 2.76 - 3 gms/cc. Hence there are four molecules contained in the unit cell.

Since first order Laue reflections are observed only from pyramidal planes (Table II) with h+k even, the space group is based on the (001) centered lattice, Γ_m'. The following space groups are derived from Γ_m':

$$C_s^3 , \quad C_s^4 , \quad C_2^3 , \quad C_{2h}^3 , \quad C_{2h}^6$$

Of these space groups only C_s^4 and C_{2h}^6 require the first order absences which were regularly observed; namely (hol) planes. Since there is no evidence to indicate the polar space group C_s^4, C_{2h}^6 is to be taken as the correct one. (This space group for muscovite has also been derived by Mauguin and by Jackson and West).

The coordinate positions for equivalent atoms provided by C_{2h}^6 are:

4a: $00\frac{1}{4}$; $00\frac{3}{4}$; $\frac{1}{2}\frac{1}{2}\frac{2}{4}$; $\frac{1}{2}\frac{1}{2}\frac{1}{4}$

4b: $0\frac{1}{2}\frac{1}{4}$; $0\frac{1}{2}\frac{3}{4}$; $\frac{1}{2}0\frac{1}{4}$; $\frac{1}{2}0\frac{3}{4}$

4c: $\frac{1}{4}\frac{1}{4}\frac{1}{4}$; $\frac{3}{4}\frac{1}{4}\frac{3}{4}$; $\frac{1}{4}\frac{3}{4}\frac{3}{4}$; $\frac{3}{4}\frac{3}{4}\frac{1}{4}$

4d: $\frac{3}{4}\frac{3}{4}\frac{3}{4}$; $\frac{1}{4}\frac{3}{4}\frac{1}{4}$; $\frac{3}{4}\frac{1}{4}\frac{1}{4}$; $\frac{1}{4}\frac{1}{4}\frac{3}{4}$

4e: $0u0$; $\frac{1}{2}, u+\frac{1}{2}, 0$; $0\bar{u}\frac{1}{2}$; $\frac{1}{2}, \frac{1}{2}-u, \frac{1}{2}$

8f: xyz ; $x+\frac{1}{2}, y+\frac{1}{2}, z$; $x, \bar{y}, z+\frac{1}{2}$; $x+\frac{1}{2}, \frac{1}{2}-y, z+\frac{1}{2}$

$\bar{x}y\bar{z}$; $\frac{1}{2}-x, y+\frac{1}{2}, \bar{z}$; $\bar{x}, \bar{y}, \frac{1}{2}-z$; $\frac{1}{2}-x, \frac{1}{2}-y, \frac{1}{2}-z$

These positions are obtained from the tabulation of Wyckoff by the cyclic permutation $x_W \sim z$, $y_W \sim x$, $z_W \sim y$. The minimum number of parameters required to determine the positions of 4 K^{+}, 8 Al^{3+}, (12 Si^{4+} + 4 Al^{3+}), 8 OH^{-}, and 40 O^{--} in the unit is fifteen. With so many parameters it is obviously impractical to deduce the atomic arrangement from X-ray data alone. It therefore becomes necessary to predict the parameter values by means of a postulated structure satisfying the general principles governing the structure of complex ionic crystals (3).

It will be later found convenient to transfer the origin of the unit cell to a center of symmetry. In this case the positions 4e above are transformed to

4E: $0u\frac{1}{4}$; $\frac{1}{2}, u+\frac{1}{2}, \frac{1}{4}$; $0\bar{u}\frac{3}{4}$; $\frac{1}{2}, \frac{1}{2}-u, \frac{3}{4}$

The eight equivalent positions become

8F: xyz ; $x+\frac{1}{2}, y+\frac{1}{2}, z$; $x, \bar{y}, z+\frac{1}{2}$; $x+\frac{1}{2}, \frac{1}{2}-y, z+\frac{1}{2}$

$\bar{x}\bar{y}\bar{z}$; $\frac{1}{2}-x, \frac{1}{2}-y, \bar{z}$; $\bar{x}, y, \frac{1}{2}-z$; $\frac{1}{2}-x, y\ \frac{1}{2}, \frac{1}{2}-z$

III. A Proposed Structure for Mica

With the aid of the general principles governing the structures of complex ionic crystals, Professor

Pauling has formulated a structure for the micas which is compatible with the space group C_{2h}^6 and the chemical composition (4).

The dimensions of the unit in the basal plane of muscovite closely approximate those for the pseudohexagonal crystal hydrargillite, $Al(OH)_3$, as well as those for the hexagonal layers in the two forms of silica, β-tridymite, and β-cristobalite. The monoclinic unit of structure of hydrargillite has $\underline{a} = 8.70$ Å, $\underline{b} = 5.09$ Å, $\underline{c} = 9.76$ Å, and $\beta = 85\ 29'$. The crystal is composed of layers of octahedra, the octahedra in each layer consisting of 6 OH^- ions grouped about an Al^{3+} ion (5). Such a layer is shown in figure 1. Each octahedron shares three edges with neighboring octahedra. The electrostatic valence rule is satisfied, since each OH^- ion is held by two bonds, each of strength $\frac{1}{2}$, the strength in this case being defined as the valence of the Al^{3+} ion divided by its coordination number.

The hexagonal layers of silicon tetrahedra present in β-tridymite and in β-cristobalite are shown in figure 2, the dimensions being $\underline{a} = 5.03$ Å, $\underline{b} = 8.71$ Å. Another type of layer having the same dimensions would be one in which all the tetrahedra point in the same direction, as shown in figure 3. The oxygen ions

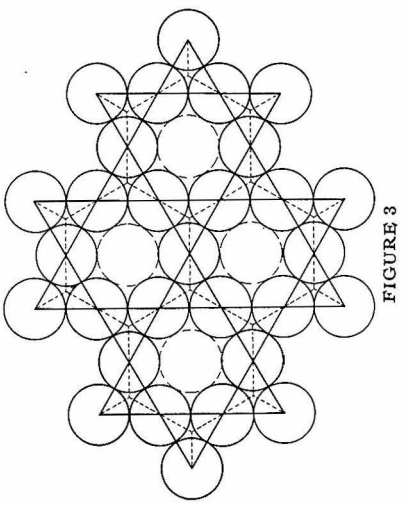

FIGURE 3

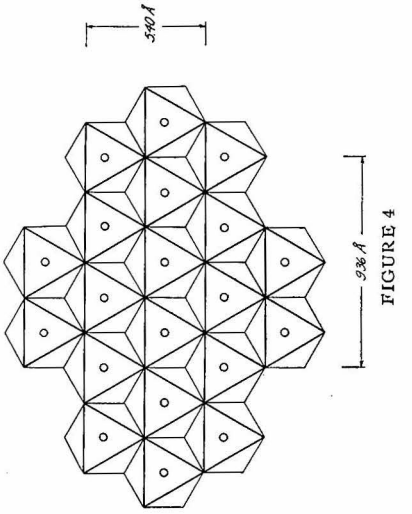

FIGURE 4

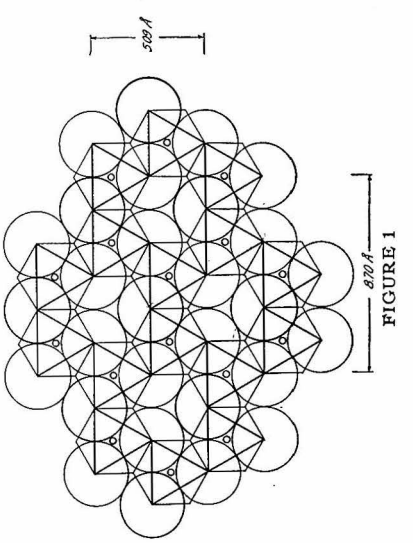

FIGURE 1

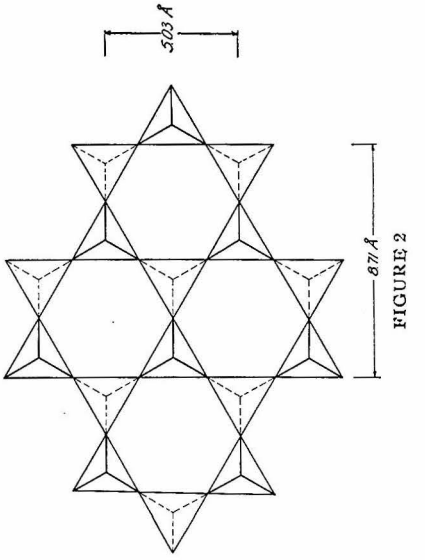

FIGURE 2

Fig. 1. A hydrargillite layer of octahedra. The light circles indicate oxygen ions, the heavier ones hydroxyl or fluorine ions in mica.

Fig. 2. A tetrahedral layer from β-cristobalite or β-tridymite. A silicon ion is located at the center of each tetrahedron, and an oxygen ion at each corner.

Fig. 3. A tetrahedral layer in which all the tetrahedra point in the same direction.

Fig. 4. A complete layer of octahedra (brucite layer).

forming the bases of the tetrahedra are held by two oxygen-silicon bonds, each of strength one, and so the electrostatic rule is satisfied for them. However the oxygen ions occupying unshared tetrahedral corners are held by only one bond of strength one, and hence it is necessary that they be held by further bonds. The distance between neighboring tetrahedron corners is $\frac{1}{3}\underline{b} = \frac{1}{3} \cdot 8.71 = 2.90$ Å. The length of an octahedral edge in hydrargillite is $\frac{\sqrt{3}}{3}\underline{a} = \frac{\sqrt{3}}{3} \cdot 5.40 = 3.12$ Å. Hence with only small distortions, these two layers can be joined in such a way that the oxygen ions occupying the unshared tetrahedron corners are coincident with two-thirds of the octahedra corners, the remaining one-third being occupied by hydroxide ions or fluoride ions. If a similar tetrahedral silica layer be attatched to the other side of the hydrargillite layer, the resultant layer would be electrically neutral and would correspond to the chemical composition $Si_4Al_2O_{10}(OH,F)_2$. The valences of all the ions would be satisfied, since the oxygen ions at the corner of a tetrahedron and two octahedra would be held by a silicon-oxygen bond of strength one, and by two aluminum-oxygen bonds, each of strength one-half. The total thickness of this layer

would be about 10 Å. It is probable that the mineral pyrophillite with this composition has this structure. Hereafter, these layers will be referred to as "pyrophillite layers".

Actually two different pyrophillite structures can be built up in the manner described, depending upon the relative positions of two tetrahedral layers joined to a hydrargillite layer. One manner of placing the tetrahedral layers puts the hydroxyl ions or fluoride ions at the ends of the shared octahedral edges. The other possibility puts the hydroxyl ions or fluoride ions at the opposite ends of the unshared octahedral edges. Both of these structures satisfy the electrostatic valence rule and correspond to the same chemical composition.

In order to obtain a structure compatible with the chemical composition of muscovite it is necessary to replace one-fourth of the silicon ions in a pyrophillite layer by aluminum ions and to regain electrical neutrality by the introduction of a corresponding number of potassium ions. Aluminum ions can have the coordination number four as well as six, and thus the substitution for silicon ions in the tetrahedral layer is possible without disrupting the structure. The potassium ions can be fitted into the cavities formed by six oxygen

ions on top of one layer and six on the bottom of the layer above. The resultant structure has the chemical composition of muscovite. The electrostatic valence rule is not entirely satisfied, since some of the oxygen ions will be held by three bonds having a total strength of $1\frac{3}{4}$. However this deviation is not serious. The pyrophillite layers are electrically negative and are held together by the electrostatic forces of the potassium ions between them.

The postulated structure for mica is not rigorously compatible with the space group C_{2h}^6 because one-fourth of the silicon ions in the tetrahedral layer are replaced by aluminum ions. The failure of the X-ray investigation to indicate lower symmetry is to be attributed to the small difference in scattering power between aluminum and silicon.

Since d_{001} in muscovite has been found to be 20.04 Å, there must be two pyrophillite layers to the unit.

IV. Testing the Predicted Structures by Observed and Calculated Intensities of Reflection.

The space group C_{2h}^6 requires that the potassium ions be located either at centers of symmetry or on two

fold rotation axes. In the former case there are two possible structures corresponding to the two possibilities described for pyrophillite. In the latter case only one structure is possible, for then the presence of centers of symmetry at the centers of the shared octahedral edges excludes the possible pyrophillite structure in which the hydroxide ions or fluoride ions are located at the ends of the unshared octahedral edges. In what follows, the three postulated structures will be designated as A, B, and C.

1. Structure A shall refer to the one in which the potassium ions are located at centers of symmetry and the two tetrahedral layers are joined to the hydrargillite layer in such a way that hydroxide ions occupy the ends of shared octahedral edges.

2. Structure B shall refer to the one in which the potassium ions are located at centers of symmetry and the two tetrahedral layers are joined to the hydrargillite layer in such a way that hydroxide ions occupy the ends of unshared octahedral edges.

3. Structure C shall refer to the one in which the potassium ions are located on two fold rotation axes, the pyrophillite layers then being the same as in structure A.

Each of the three structures has the following sequence of atom-planes normal to (001):

Ions	z coordinate
4 Al^{3+}	0
4 O^{--} + 2 (OH^-,F^-)	z_1
3 Si^{4+} + Al^{3+}	u
6 O^{--}	z_2
2 K^+	$\frac{1}{4}$
6 O^{--}	$\frac{1}{2} - z_2$
3 Si^{4+} + Al^{3+}	$\frac{1}{2} - u$
4 O^{--} + 2 (OH^-,F^-)	$\frac{1}{2} - z_1$
4 Al^{3+}	$\frac{1}{2}$
4 O^{--} + 2 (OH^-,F^-)	$\frac{1}{2} + z_1$
3 Si^{4+} + Al^{3+}	$\frac{1}{2} + u$
6 O^{--}	$\frac{1}{2} + z_2$
2 K^+	$\frac{3}{4}$
6 O^{--}	$- z_2$
3 Si^{4+} + Al^{3+}	$- u$
4 O^{--} + 2 (OH^-,F^-)	$- z_1$
4 Al^{3+}	0

Inasmuch as all three structures, A, B, and C have the same sequence of atom planes along the normal to (001), the calculated intensities of reflection of (00ℓ) planes will be the same. Hence a comparison of observed and calculated intensities for (00ℓ) will serve to determine the essential correctness of the postulated structures. For simplicity in calculation an"ideal" structure is assumed, that is, all the tetrahedra and octahedra are assumed to be regular, although this would doubtlessly not be the case in the actual structure. The intensities of reflection will then be dependent only upon three parameters determining the spacing of the atom planes. The intensities of reflection of (00ℓ) planes are calculated from the formula

$$I = \text{constant} \cdot A^2 , \qquad (1)$$

where $A = \sum_n A_n e^{2\pi i \ell z_n}$, the summation being taken over all the atoms in the unit.

$$A_n = \left(\frac{1 + \cos^2 2\theta}{2 \sin 2\theta}\right)^{\frac{1}{2}} F_n$$

F_n denotes the atomic scattering factor for the nth atom in the unit. The F factors employed in subsequent calculations are taken from a tabulation by Bragg and West (6). The corresponding A values are given in Table III. The quantity A^2 must approximately parallel the estimated intensities of reflection on any one photograph.

TABLE III

Amplitude Factors for Oxygen, Aluminum, Silicon, and Potassium

d (Å)	O	Al	Si	K
0.5	0.1	1.1	1.3	2.2
0.6	0.2	1.7	2.0	3.2
0.8	1.0	3.4	4.2	5.5
1.0	2.0	5.2	6.0	7.9
1.2	3.2	7.0	7.9	10.2
1.4	4.3	8.7	9.7	12.5
1.6	5.4	10.3	11.3	14.8
1.8	6.5	11.8	12.8	17.0
2.0	7.6	13.3	14.5	19.2
2.2	8.8	14.8	15.9	21.4
2.4	9.9	16.2	17.3	23.5
2.6	11.0	17.5	18.6	25.5
2.8	12.0	18.9	20.0	27.4
3.0	13.0	20.0	21.2	29.3
3.2	14.0	21.2	22.4	31.1
3.4	15.0	22.3	23.5	32.9
3.6	15.9	23.2	24.5	34.5
3.8	16.8	24.1	25.5	36.2
4.0	17.6	25.0	26.4	37.8

Table III Continued

d (Å)	O	Al	Si	K
4.2	18.5	25.8	27.2	39.4
4.4	19.2	26.5	27.9	40.9
4.6	20.0	27.2	28.6	42.4
4.8	20.6	27.8	29.2	43.8
5.0	21.2	28.4	29.8	45.2

Assuming the thickness of the octahedral layer to be the same as found for it in hydrargillite and the tetrahedra to be 2.60 Å on an edge, the parameter values $z_1 = 0.055$, $u = 0.137$, $z_2 = 0.165$ were predicted.

The amplitude expression for the planes (00ℓ) is

$$A = 2A_{Al} + (-1)^{\frac{\ell}{2}} A_K + (3A_{Si} + A_{Al})\cos 2\pi\ell u + 6A_O(\cos 2\pi\ell z_1 + \cos 2\pi\ell z_2),$$

with ℓ having even values. The structure factor for OH^- ion or F^- ion was taken to be the same as for O^{--} ion.

The observed intensities were obtained by a visual comparison of four photographs from fuchsite, identical except for varying exposure times of 15, 90, 300, and 960 minutes. Because of the large value of d_{001} (20.04 Å), reflections as high as the thirty sixth order were observed. Table IV tabulates the calculated and observed intensities. The constant in equation (1) was given the arbitrary value 0.015. The observed intensity for (002) was arbitrarily taken to be equal to the calculated intensity. The excellent general agreement serves to substantiate the proposed structure and to verify the values of the predicted parameters.

In order to determine which, if any, of the three structures A, B, or C is correct, it is necessary to calculate the intensities of reflection involving the x and y parameters. In these calculations the ideal

Table IV

Comparison of Observed and Calculated Intensities of Reflection of (00ℓ) Planes

X-rays incident on (001) a axis vertical

Oscillation 0° - 45°.

(00ℓ)	Observed Intensity	Calculated Intensity
002	40	40
004	40	47
006	120	121
008	20	18
00·10	150	124
00·12	3	7
00·14	10	12
00·16	30	30
00·18	0.5	1.4
00·20	6	4.3
00·22	9	4.5
00·24	2	4.8
00·26	2	5.2
00·28	0	0.0
00·30	0.8	1.6
00·32	0.1	0.2
00·34	0	0.6
00·36	1	1.7

structures are assumed and the z parameters discussed above are employed.

For structures A and B the orientation of the unit cell is chosen so that the eight general positions defined by the space group are those given by 8f and which have been previously tabulated. For structure C the origin of the unit cell is transferred to a center of symmetry so that the eight general positions are given by 8F. From the geometry involved in the planes parallel to (001) the following "ideal" parameters are predicted for each structure:

Structure A

4 K^+ ions in 4d positions

8 Al^{3+} ions in two sets of 4e positions with $u_1 = 7/12$, $u_2 = 11/12$.

12 Si^{4+} + 4 Al^{3+} in two sets of 8f postions

$x_1 = 0.211$	$y_1 = 1/12$	$z_1 = 0.137$
$x_2 = 0.211$	$y_2 = 5/12$	$z_2 = 0.137$

8 OH^- ions in 8f positions

$x_3 = 0.685$	$y_3 = \frac{1}{4}$	$z_3 = 0.055$

40 O^{--} ions in five sets of 8f positions

$x_4 = 0.135$	$y_4 = 1/12$	$z_4 = 0.055$
$x_5 = 0.135$	$y_5 = 5/12$	$z_5 = 0.055$
$x_6 = 0.222$	$y_6 = \frac{1}{4}$	$z_6 = 0.165$
$x_7 = 0.972$	$y_7 = 0$	$z_7 = 0.165$
$x_8 = 0.472$	$y_8 = 0$	$z_8 = 0.165$

Structure B

4 K^{+} ions in 4c positions

8 Al^{+++} ions in two sets of 4e positions with $u_1 = 5/12$ and $u_2 = \frac{3}{4}$.

12 Si^{4+} + 4 Al^{3+} in two sets of 8f positions

$x_1 = 0.211$ $y_1 = 7/12$ $z_1 = 0.137$

$x_2 = 0.211$ $y_2 = 11/12$ $z_2 = 0.137$

8 OH^{-} ions in 8f positions

$x_3 = 0.185$ $y_3 = \frac{1}{4}$ $z_3 = 0.055$

40 O^{--} ions in five sets of 8f positions

$x_4 = 0.685$ $y_4 = 1/12$ $z_4 = 0.055$

$x_5 = 0.685$ $y_5 = 5/12$ $z_5 = 0.055$

$x_6 = 0.472$ $y_6 = 0$ $z_6 = 0.165$

$x_7 = 0.722$ $y_7 = \frac{1}{4}$ $z_7 = 0.165$

$x_8 = 0.972$ $y_8 = 0$ $z_8 = 0.165$

Structure C

4 K^{+} ions in 4 [illegible] with u = 1/12

8 Al^{3+} ions in 8 F with

$x_1 = \frac{1}{4}$ $y_1 = 1/12$ $z_1 = 0$

12 Si^{4+} + 4 Al^{3+} in two sets of 8 F postions

$x_2 = 0.961$ $y_2 = \frac{3}{4}$ $z_2 = 0.137$

$x_3 = 0.961$ $y_3 = 5/12$ $z_3 = 0.137$

8 OH^{-} ions in 8 F positions

$x_4 = 0.935$ $y_4 = 1/12$ $z_4 = 0.055$

40 O^{--} ions in five sets of 8 F positions

$x_5 = 0.935$	$y_5 = \frac{3}{4}$	$z_5 = 0.055$
$x_6 = 0.935$	$y_6 = 5/12$	$z_6 = 0.055$
$x_7 = 0.472$	$y_7 = 1/12$	$z_7 = 0.165$
$x_8 = 0.222$	$y_8 = 1/3$	$z_8 = 0.165$
$x_9 = 0.222$	$y_9 = 5/6$	$z_9 = 0.165$

Inasmuch as there is no reason, a priori, to prefer any particular arrangement of the aluminum ions in the tetrahedral layers, it has been assumed in the intensity calculations that the two sets of 8f positions containing the 12 Si^{4+} and 4 Al^{3+} in the unit each contain 6 Si^{4+} and two Al^{3+}. Since the structure factors for aluminum and silicon are not greatly different, this assumption will not cause any serious change in the relative values of the calculated intensities.

In the attempt to eliminate two of the three possible structures the intensities of reflection of (0k0) planes will first be calculated and compared with the observed values. The calculated values depend only upon the y parameters. The experimental values were obtained visually from an oscillation photograph prepared with the molybdenum K_α lines isolated by means of a zirconia filter. The crystallographic c axis was made the axis of rotation. The data are tabulated in Table V.

Table V

Comparison of Observed and Calculated Intensities of Reflection of (0k0) planes for Structures A, B, and C.

Photograph 1. X-rays incident on (010), c axis vertical. oscillation 0° - 45°. 400 milliampere hours.

(0k0)	I_A	I_B	I_C	$I_{observed}$
020	640	160	1	10
040	83	260	140	15
060	865	865	865	80
080	3	23	30	10
0·10·0	11	2	1	1
0·12·0	115	115	115	20
0·14·0	2	0	0	0
0·16·0	0	7.6	0	0
0·18·0	1	1	1	0

An inspection of the table shows that the agreement is not striking in any of the three cases. Moreover, in each case the relative values of the calculated intensities disagree with the observed values to approximately the same extent, so that the elimination of any one structure is not possible on the basis of these results. In all cases the relative values of the (020) intensities are rather seriously in error. The relative values for all other planes parallel the observed values satisfactorally. Instead of attempting to vary the parameters

so as to obtain better agreement, the intensities of reflection of other planes will be calculated and compared with experiment. The next set of planes which would be reasonable to try would be the (h00) planes. However the calculated values come out the same in all three cases, so that here again no useful information concerning the probable correctness of any one of the structures can be obtained. The next set of planes selected for study are those of the type (0kℓ), ℓ even. The relative values of the observed intensities are taken from the same photograph used previously. Table VI tabulates the results. The observed intensities are multiplied by the factor ω in order to correct for the varying specific times of illumination of planes inclined to the axis of rotation.

Table VI

Comparison of Observed and Calculated Intensities of (0kℓ) planes for Structures A, B, and C.

(0kℓ)	I_A	I_B	I_C	$\omega \cdot I_{observed}$
022	154	1	36	15
024	472	1000	450	40
026	660	300	20	5
042	320	120	4	20
044	7	82	61	25
046	1	37	30	20

The data in this table show that there is sufficient disagreement between calculated and observed intensities for structures A and B to indicate that these structures are quite probably incorrect. Since the actual structure, is, of course, not derived from perfectly regular octahedra and tetrahedra, it is not justifiable to eliminate A and B until the effect of variation of parameters on the calculated intensities is determined. It is found on calculation that no reasonable distortions of the ideal structures A and B can significantly improve the agreement between relative calculated and observed intensities for the planes tabulated in Table VI. The reverse is the case for structure C. Before definitely concluding that C is the correct structure, the intensities of reflection of many additional planes were calculated for all three structures and it was found that the same sort of disagreement prevailed for A and B as was found previously. In no case were the relative values for A and B in better agreement with the observed than for C. Hence structure C is to be accepted as the correct one.

Since there are eighteen x and y parameters in structure C it is obviously impossible to try to fix their values more accurately than the predicted ones by

independently varying them. Inasmuch as it is known that in hydrargillite the shared octahedral edges are shortened from 2.90 Å in the ideal case to 2.50 Å, it seems reasonable to suppose that this is also the case in mica. Introducing the length of a shared octahedral edge as a parameter and assuming that the length of the edge may only vary in such a way as to leave the z parameters unaltered, it was found that the best agreement was obtained when the length of the shared edge is taken to be 2.64 Å as compared to 3.00 Å in the ideal case. The calculated and observed intensities for all planes investigated are tabulated in Tables VII and VIII. I_C and I'_C denote the calculated intensities for the ideal structure and the distorted structure (shared octahedral edges 2.64 Å) respectively. Observed intensities are given on an arbitrary scale. Although the agreement between I'_C and $\omega \cdot I_{observed}$ is by no means completely satisfactory, it is sufficient to establish the structure. Intensities were calculated for approximately eighty five prism reflections. No pyramidal planes were used for the reason that the calculations, dependent upon all the twenty eight x, y, and z parameters simultaneously, become too laborious and are not essential to establishing the structure. The final parameter values

Table VII

Comparison of Calculated and Observed Intensities

Photograph 1. Incident X-rays on (010) c axis vertical. Oscillation 0°-45°.

(hkl)	I_c	I'_c	$\omega \cdot I_{observed}$
020	1	12	10
021	84	84	10
022	36	72	15
023	300	300	20
024	450	470	40
025	560	560	50
026	30	30	5
027	54	54	10
028	20	10	5
029	7	7	10
02·10	23	14	10
02·11	4	4	5
02·12	40	34	10
02·13	45	45	20
040	140	67	15
041	150	150	20
042	4	21	20
043	96	96	20
044	61	52	25

Table VII Continued

(hkl)	I_c	I'_c	$\omega \cdot I_{observed}$
045	1	1	0
046	30	46	20
047	37	37	15
048	1	6	5
049	1	1	0
04·10	1	4	5
04·11	96	96	10
04·12	88	100	15
04·13	200	200	25
04·14	6	7	5
060	870	820	80
061	0	0	1
062	65	56	10
063	0	0	0
064	13	1	0
065	0	0	0
066	1	1	1
067	0	0	0
068	130	150	20
069	0	0	10
06·10	92	84	15

Table VII Continued

(hkl)	I_C	I'_C	$\omega \cdot I_{observed}$
06·11	0	0	0
06·12	7	6	0
06·13	0	0	5
06·14	75	74	10
080	15	30	10
0·10·0	1	1	0
0·12·0	120	100	20
0·14·0	1	1	0
0·16·0	1	1	0
0·18·0	10	9	0

Table VIII

Comparison of Calculated and Observed Intensities

Photograph 2. Incident X-rays on (100) c axis vertical

Oscillation $0^{\circ}-45^{\circ}$. 400 milliampere hours

(hkl)	I_C	I'_C	$\omega \cdot I_{observed}$
200	640	620	40
202	82	75	30
204	14	13	10
206	200	210	30
208	77	78	20
20·10	340	330	35
20·12	420	410	50
$20\bar{2}$	680	670	60
$20\bar{4}$	720	740	50
$20\bar{6}$	380	390	40
$20\bar{8}$	9	8	5
$20\cdot\bar{1}0$	770	770	50
$20\cdot\bar{1}2$	19	19	10
400	390	400	50
600	7	15	10

Table IX

Atomic Coordinates in Muscovite

4 K^{+} ions in 4 E positions with u = 1/12

8 Al^{3+} ions in 8 F positions with

$x_1 = \frac{1}{4}$ $y_1 = 1/12$ $z_1 = 0$

12 Si^{4+} + 4 Al^{3+} ions in two sets of 8 F positions

$x_2 = 0.961$ $y_2 = \frac{3}{4}$ $z_2 = 0.137$

$x_3 = 0.961$ $y_3 = 5/12$ $z_3 = 0.137$

8 OH^{-} ions in 8 F positions

$x_4 = 0.948$ $y_4 = 0.070$ $z_4 = 0.055$

40 O^{--} ions in five sets of 8 F positions

$x_5 = 0.910$ $y_5 = \frac{3}{4}$ $z_5 = 0.055$

$x_6 = 0.948$ $y_6 = 0.430$ $z_6 = 0.055$

$x_7 = 0.472$ $y_7 = 1/12$ $z_7 = 0.165$

$x_8 = 0.222$ $y_8 = 1/3$ $z_8 = 0.165$

$x_9 = 0.222$ $y_9 = 5/6$ $z_9 = 0.165$

are given in table IX. The z parameters, determined from eighteen even orders of reflection of (001) planes are probably accurate to within 0.005 Å. The x and y parameters are probably correct to within 0.05 Å.

V. Some Remarks Concerning the Structure

A photograph of a model of the structure is given in figure 5. The two pyrophillite layers in the unit are related to each other by means of two fold axes in planes mid-way between them.

The O^{--}, OH^{-}, and F^{-} ions in the octahedral layers are arranged in a plane in hexagonal close packing. The oxygen ions forming the bases of the tetrahedra occupy three of the four positions of a close packed plane, the fourth position being indicated by the dotted circle in figure 3.

The structure for muscovite leads to a general chemical formula for the micas (7), (8):

$$KX_nY_4O_{10}(OH,F)_2 \qquad 2 \leq n \leq 3$$

X represents cations which may have the coordination number six, (Al^{3+}, Mg^{++}, Fe^{++}, Fe^{3+}, Mn^{++}, Mn^{3+}, Ti^{4+}, Li^{+}, etc) and Y cations of coordination number 4 (Si^{4+}, Al^{3+}, etc) The value n = 2 corresponds to a hydrargillite layer of octahedra while the value three corresponds

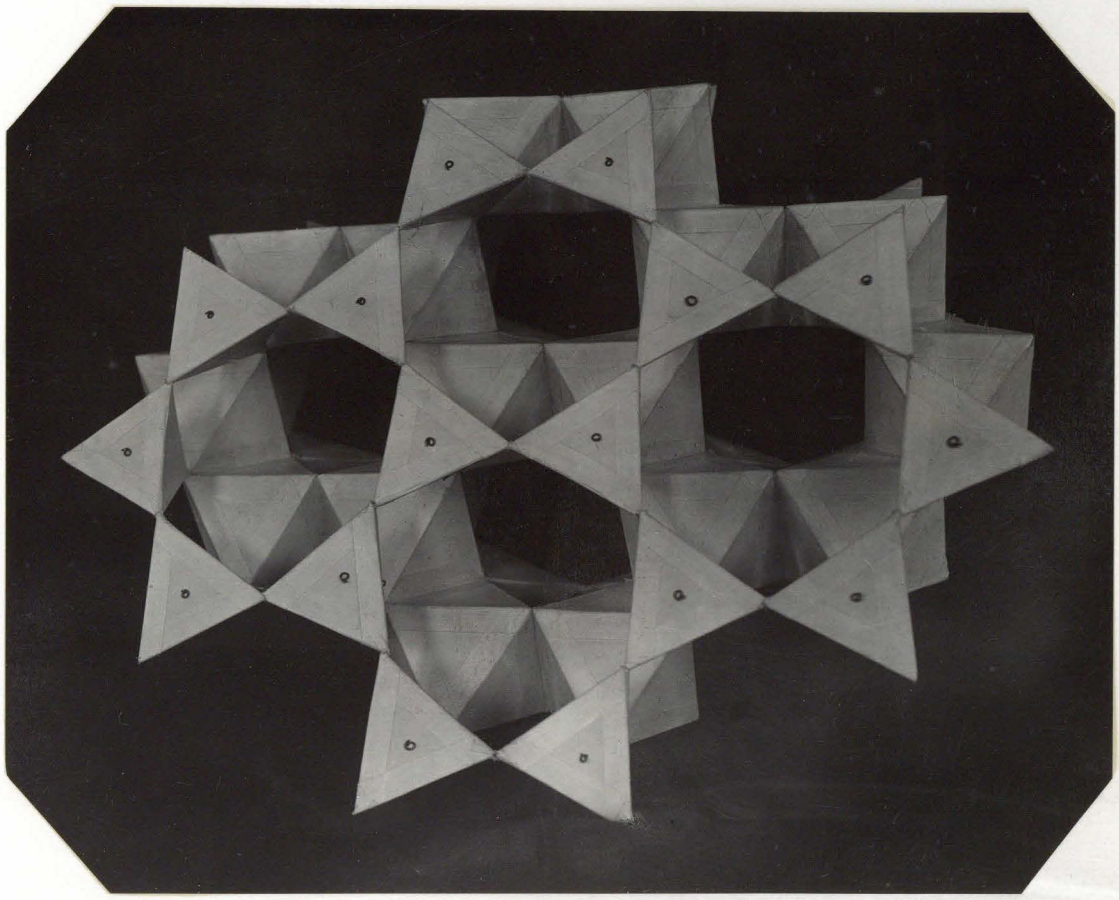

Fig. 5. A model representing the structure of mica

to a completed octahedral layer (figure 4). The distribution of the various X and Y ions must be such as to satisfy the electrostatic valence rule as much as possible.

Summary

A crystal of muscovite, $KAl_3Si_3O_{10}(OH)_2$, was analyzed by means of Laue and rotation photographs and was found to have a monoclinic unit of structure of dimensions $\underline{a} = 5.23$ Å, $\underline{b} = 9.09$ Å, $\underline{c} = 20.14$ Å, $\beta = 96°$. The unit contains four molecules. The space group is C_{2h}^6. With the aid of the coordination theory of close packing a number of structures were devised having the observed unit and symmetry (4). One of these was shown to explain the intensities observed on the oscillation photographs.

The structure is composed essentially of octahedra of oxygen and hydroxyl ions about a metal ion (aluminum) and of tetrahedra of oxygen ions about a metal ion (silicon). These octahedra and tetrahedra are arranged in the manner indicated by the model shown in figure 5.

I wish to acknowledge my appreciation to Professor Linus Pauling for encouragement, advice, and direction in the studies here reported.

References

1. Ch. Mauguin, Comp Rend, 185, 288, (1927)
2. W. Jackson and J. West, Z Krist., 76, 211 (1931)
3. L. Pauling, J. Am Chem Soc. 51, 1010, (1929)
4. L. Pauling, Proc Nat Acad Sci., 16, 123 (1930).
5. L. Pauling, to be published in the Z. Kristallographie.
6. W.L.Bragg and J. West, Z Krist., 69, 139, (1928)
7. This formula has been deduced by Professor Pauling, reference 4.
8. This formula is in agreement with the accurate chemical analyses of over fifty mica specimens reported by J. Jakob, Z Krist., 61, 155 (1925); 62, 443 (1925); 69, 217, 403, 511, (1928-9); 70, 493, (1929); 72, 329 (1930)